Norwegian University
of Life Sciences

Master's Thesis 2024 45 ECTS
Faculty of Environmental Sciences and Natural Resource Management

Estimating collision risk for white-tailed eagles (*Haliaeetus albicilla*) in onshore wind power environments – Application of spatial modelling frameworks and predictive mapping

Gjermund Sandvik Halgunset
Natural Resource Management

Preface

This thesis marks the end of a double bachelors run in Renewable Energy and Ecology and Natural Resource Management, and a master's degree in Natural Resource Management. The thesis is written on behalf of the Norwegian Institute of Nature Research (NINA) and expands the horizon of previous impact research from Smøla wind farm. During my time as a student at Norwegian University of Life Sciences (NMBU), I have been lucky enough to explore a large variety of complex issues related to renewable energy and nature conservation. Therefore, this thesis is a well fitted ending to what I would consider as six engaging and eventful years at NMBU.

First and foremost, I would like to show my appreciation for Ronny Steen, my main supervisor from NMBU through this adventure. The guidance from Ronny has been consistent through the entire process, and he has been particularly important in helping me with the statistical modelling. I would also like to express my deepest gratitude to my supervisors at NINA, Roel May and Diego Pavòn-Jordàn, for allowing me to embark on this project. This thesis has given me the opportunity to shed an additional light on the need for a balanced relationship between renewable energy installations and nature conservation efforts. Roel and Diegos knowledge and experience with collision risk modelling has been essential for my progress. I would also like to extend my gratitude to all my friends and family for their constant support. A special thanks to the men's choir Over Rævne and Samfunnet in Ås for making my time as a student nothing less than phenomenal.

Norwegian University of Life Sciences

Ås, 14.05.2024

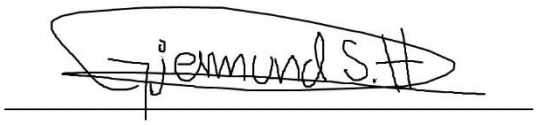

Gjermund Sandvik Halgunset

Abstract

Although wind power has proven to be a key component in the efforts of fighting climate change, their harmful effects on avian wildlife has raised increasingly prominent concerns. As the development of wind power is expected to continue at a faster pace, the potential increase in fatal bird collisions is immense. Large-bodied, soaring birds are known to be particularly at risk, for which the White-tailed Eagle (*Haliaeetus albicilla*) is quintessential.

In this study, the collision risk for white-tailed eagles were predicted and extrapolated to the entire landscape of central and northern Norway (i.e. mapping their landscape of risk). The predictions were based on satellite telemetry data, showing the wide-ranging movements patterns of 34 sub-adult individuals. Their total predicted collision risk across the landscape was found by combining the results of three predictive models, including their resource selection, their risk flight height (50 – 185 m), and a mathematical model centered on direct collision risk. Furthermore, the final predictive collision risk maps were used to assess the collision risk of existing wind farms within the study area. During their movements along the coast, white-tailed eagles are also prone to cumulative effects of several wind farms. Hence, the movement trajectories of each eagle were used to estimate the cumulative collision risk based on the risk levels of each intersected wind farm.

The resource selection revealed that white-tailed eagles were most likely to appear in sparsely vegetated, coastal lowlands. They also favored steep slopes, which aligns nicely with their exploitation of orographic uplift for soaring flight. The probability of flying at risk heights also increased in slopes, while the direct collision risk was more evenly distributed across the landscape. The total predicted collision risk based on all model results was notably higher in the steep coastal landscapes along the Norwegian fjords and declined rapidly with increasing topographic elevation. For the risk posed by each wind farm, the size had a considerable effect on total collision risk, which was expected. However, the findings also revealed that certain smaller wind farms were sited less effectively within preferable eagle habitats. In the cumulative collision risk assessment, the risk varied greatly between individuals, with certain individuals avoiding wind farms more effectively than others. Some individuals also avoided high risk wind farms more effectively, despite moving through the same number of wind farms in total.

Predictive collision risk modelling and cumulative risk assessments represents an advancement towards limiting the harmful effects of wind power. Facilitating the opportunity to analyze predicted collision risk over large areas can improve the effectiveness of strategic planning and site selection. Moreover, by assessing the collision risk in existing wind farms and their cumulative effects on white-tailed eagles, additional site-specific mitigation strategies can be implemented as needed. If not addressed properly, the ecological implications of wind power can be extensive. However, these methods and findings can improve the knowledge base related to birdlife protective practices and future wind power developments in general.

Table of contents

1. Introduction

Over the past few decades, wind power has become an increasingly competitive contributor in the global energy production. Wind power creates clean and emission-free energy outputs, limiting the overall greenhouse gas emissions from the energy sector (Abbasi et al., 2013; Vargas et al., 2019). As a result of enhanced technology and low production costs, the Intergovernmental Panel for Climate Change (IPCC) suggest that wind power will amount to 20 % of the global energy demand in the runup to 2050 (Abbasi et al., 2013). However, in the case of human activities and social developments, conflicts often arise in regards to ecological conservation interests (Young et al., 2005). Despite wind power's central role in phasing out the use of fossil fuels, it entails undisputed negative consequences for the functionality of ecosystems and poses a direct threat to a number of bird species (Heuck et al., 2019). The deployment of wind farms in natural areas has exceeded the speed of the development linked to studies of how strongly wind power affects bird life (Drewitt & Langston, 2006). This increases the need for further understanding of the negative impacts that can be used as a basis for future project developments.

Among previous studies, there is a broad consensus that wind power have a negative impact on local raptor populations in the form of direct collision risk with rotating turbine blades and the towers themselves (Beston et al., 2016; Dahl et al., 2013; Drewitt & Langston, 2006; Heuck et al., 2019; Martínez et al., 2010; May et al., 2010; May et al., 2011). Moreover, the development of wind power can cause an extensive degradation of natural habitats, which is one of the main contributors to the fragmentation and destruction of key food and nesting biotopes (Beston et al., 2016; Heuck et al., 2019). The wind farms can also rise a barrier effect, causing the birds to avoid areas with high turbine densities. This can extend the flight distance and increase the energy required to fly between important feeding, nesting, and roosting sites (Drewitt & Langston, 2006). In other words, the wind power's impact on bird life includes both direct and indirect negative effects, threatening the populations of several bird species.

When studying the harmful effects of wind power development in relation to birdlife, the White-tailed Eagle (*Haliaeetus albicilla*) is particularly favorable for risk modelling due to their vulnerability in the face of wind turbines (May et al., 2013). The White-tailed Eagle is the largest bird of prey in the European fauna, with a wingspan that often reaches 2.5 meters (Barth & Gjershaug,

2023). They are also known for their long life span with a generally low reproductive rate. Most individuals do not lay their first eggs until they are 5-6 years old, and only 1-2 eggs are usually laid per breeding season (Kroglund, 2022). In this way, white-tailed eagles can be particularly vulnerable to small and sudden rises in mortality rates, increasing the risk of local population size decline (Drewitt & Langston, 2006; Heuck et al., 2019). Hence, an increase in the development of wind farms can have a harmful effect on certain populations of white-tailed eagles. Furthermore, wide-ranging bird species, such as the White-tailed Eagle, are highly prone to cumulative effects of several wind power installations (Brabant et al., 2015; Drewitt & Langston, 2006; Vasilakis et al., 2017). GPS-tracking records from the Norwegian Institute for Nature Research (NINA) have shown that young males can cover large areas over a short period (Stokmo, 2021), increasing the chances of movement patterns overlapping with several existing wind power sites. Wind farms located in migration routes are also known to increase collision risk (Kikuchi, 2008). Hence, the wide-ranging movements of white-tailed eagles along coastal habitats which are also favorable for wind power development, increase the spatial cumulative risk of collision. Therefore, with the use of GPS-data and spatial modelling, additional studies highlighting the harmful effects of existing wind farms are needed for accurate environmental impact assessments.

To further stress their vulnerability, white-tailed eagles have also shown lack of behavioral responses to avoid high density wind turbine areas, increasing the risk of collision (Dahl et al., 2013; Grünkorn et al., 2017; Krone & Treu, 2018). However, a successful attempt was made in Scotland to drive golden eagles (*Aquila chrysaetos*) away from a wind farm by felling a nearby forestry plantation. This ensured that the overall loss of foraging habitats caused by the wind farm construction were minimized. Though it is worth noting that this behavioral change was only observed in a single breeding pair, limiting the certainty of whether this measure will have a transferable effect to other sites or species (Walker et al., 2005). In many cases, the risk of increased collision occurrences is not only caused by individual factors, but rather the synergy of several drivers. Heuck et al., (2019) stated that the risk of collision for white-tailed eagles increased with a higher density of wind turbines. Additionally, an amplified effect of the turbine density occurred when the turbines were placed in highly preferable habitats. The results also suggested that the interaction of habitat suitability and turbine density was a better predictor of collision risk than the interaction of nesting site densities and turbine densities (Heuck et al., 2019). This suggests that using habitat preference in combination with turbine locations is an effective method for highlighting areas of collision risk.

White-tailed eagles are prime examples of soaring raptors, by which their flight behavior mostly revolve around the use of upward air currents to gain height (Dahl et al., 2013; Spaar, 1997). This technique is highly effective in terms of energy use, especially for large raptors. By using alternate flight methods such as flapping, their heavy body mass will cause large increase in energy consumption, compared to soaring (Spaar, 1997). The soaring technique is also effective in maintaining flight altitudes with minimized energy consumption. Dahl et al., 2013 suggest that flight altitude is an important factor in the assessment of collision risk, as the altitudes are expected to change in proximity to wind turbines. Such behavioral changes increase the need to further assess the movement patterns in relation to wind farms, and subsequently propose effective mitigation measures. Moreover, by analyzing both the eagles' habitat preferences and their flight altitudes in relation to turbine collision risk, their landscape of risk can be modelled and predicted over larger areas.

There are several methods for modeling the spatially explicit collision risk for eagle populations. The use of direct observations from different vantage points is the method used in previous studies from Smøla wind farm (Dahl et al., 2013; May et al., 2010). This provides a wide range of location-specific activity data, including flight altitude, social behavior and how local weather condition affects flight behavior (Dahl et al., 2013; May et al., 2010). Although observational methods can provide accurate information for analyzing collision risk, these data are usually limited to specific wind power projects and does not include the eagles' wide-range movements. Observer data are also prone to uncertainties related to estimates of flight height and activity due to personal observation errors and lack of sufficient acuity skills (Madders & Whitfield, 2006). Therefore, tracking flight activity from GPS-tagged individuals is a more effective method for modeling the landscape of risk and cumulative collision risk over larger areas, covering several wind power locations. Moreover, the development of wind farms in coastal regions also have a displacement effect on local eagle populations, driving them away from their traditional territories (Garvin et al., 2010; May et al., 2013). This may increase the hazards of encountering other wind farms along their displacement paths, possibly increasing the cumulative collision risk. Hence, modelling the landscape of risk for white-tailed eagles based on GPS-data can provide useful insight to how the risk accumulates depending on their movement patterns.

This thesis assesses the spatial distribution of the predicted collision risk of white-tailed eagles with wind turbines, and how this risk can be predicted using GPS-data and spatial modelling frameworks.

The main research objective is to map the spatially explicit predicted collision risk for sub-adult white-tailed eagles across the landscape by combining the results of three predictive models. These models include the predicted probabilities of presence (resource selection), predicted probabilities of flying at risk heights, and a mathematical model highlighting direct collision risk. The second objective is to assess the collision risk of existing wind farms, and their subsequent cumulative collision risk effects for white-tailed eagles along their movement trajectories. This research intends to offer actionable insights that could guide the placement and design of future wind farms to mitigate the impact on white-tailed eagles, contributing to both renewable energy development and wildlife conservation.[1]

2. Materials and methods

2.1 Study area

The modelling was conducted over the range of the GPS-tagged white-tailed eagles, from Kristiansund in the county of Møre of Romsdal (central Norway) to Båtsfjord in Finnmark (northern Norway) (Fig. 1). The tagging of nestling was carried out on the island of Smøla, which is home to one of the largest wind farms in Norway. Many sub-adult individuals have shown patterns of northern movements along the coast towards the tip of northern Norway. Along this stretch of around 1400 kilometers, the dispersing individuals will pass several existing wind farms within a matrix of coastal and inland landscapes.

[1] This introduction is based on the mandatory thesis description written in the preparatory master's course "MINA310 - Methods in Natural Sciences" (Halgunset, 2023).

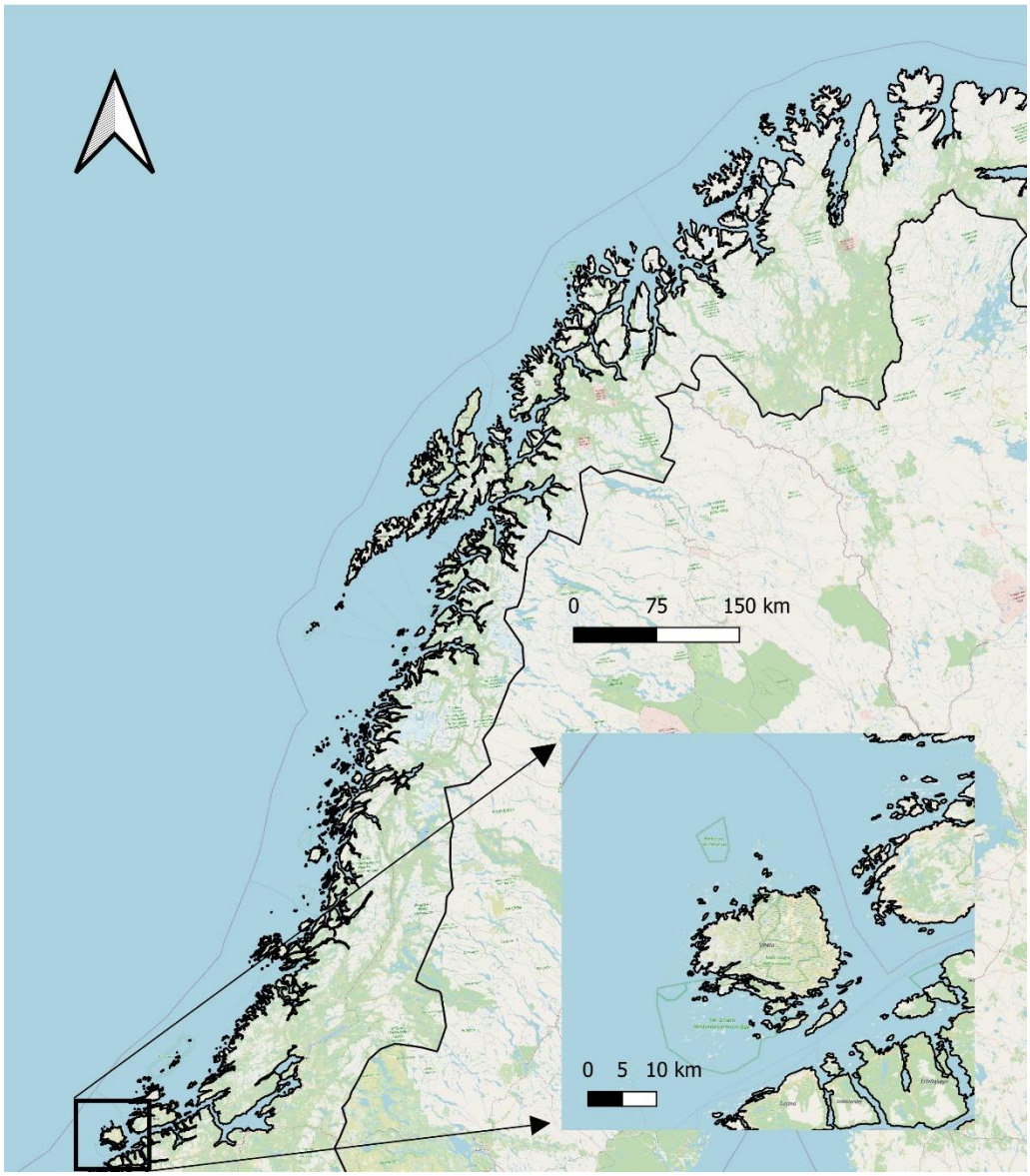

Figure 1: Study area covering the entire central and northern Norway. The highlighted area represents Smøla archipelago, where the nestlings were tagged.

2.2 Data collection

2.2.1 GPS-data

Between 2004 and 2017, NINA acquired an extensive tracking dataset of GPS-tagged white-tailed eagles fledged on the island of Smøla (Hanssen et al., 2020). The data show the spatially explicit distribution of individuals in the landscape as well as their activity. The GPS-trackers were fitted as back-packs on nestlings just prior fledging, and most were equipped with solar panels to charge the batteries. Hence, most locations were recorded between March and October due to the lack of solar radiation during the late autumn and winter (May et al., 2013). Moreover, the intervals at which

locations were registered also varied among the seasons, using short time intervals (< 1-3 hours) in the summer, 3-6 hours during autumn and spring, and up to 24 hour intervals during the winter (Nygård et al., 2010). The median tracking interval between two consecutive locations across all individuals was 15 minutes and 6 seconds. The lowest tracking interval was 39 seconds, while the highest was 24 hours. Flight altitude and flight speed data were also recorded for most tagged individuals, indicating whether the eagles were roosting/foraging or flying at the time of registration (Nygård et al., 2010). The GPS data have been used in previous collision risk studies at Smøla (May et al., 2011; Nygård et al., 2010). However, only the tracking data within Smøla wind farm was assessed, and the northern movement patterns were excluded.

2.2.2 Environmental data

The data needed for the analysis consisted in several types of environmental data, including general land cover and different types of topographic variables. The habitat categories used as explanatory variables were provided through Corine Land Cover data, available at the Norwegian Institute of Bioeconomy Research (NIBIO, 2024). The data consists of 44 different categories and constitutes a joint compilation of land cover maps from European countries. For the analysis in this thesis, the habitat categories were aggregated into more general and manageable categories, as shown in Appendix A. Moreover, a nationwide digital terrain model (DTM) in raster format was downloaded from Høydedata (Kartverket, 2023). The DTM was further used as input to generate three additional topographic raster maps containing the slope level and ruggedness of the terrain, and the topographic position index (TPI). These maps were generated using raster terrain algorithms in QGIS desktop version 3.28 (QGIS.org, 2024). The slope shows the level of steepness in the terrain, while the ruggedness shows the general level of unevenness. The TPI indicates weather a position is in a valley or at a hilltop. Wind power locations and wind speed data was provided by the public databases of The Norwegian Water Resources and Energy Directorate (NVE, 2024b).

2.3 Data handling and preparation

2.3.1 Data filtering

The extensive raw dataset from NINA provided a significant number of eagle relocations of different quality. Considering that the GPS-transmitters were fitted on nestlings, large amounts of registrations

were made in the pre-fledging phase in the nest and in the post-fledging dependency phase (PFDP). This could bias the utilization distribution and cause inaccurate home range estimations. The PFDP is the period after fledging used for exploration and skill development near the natal site. The phase usually last between 1-2 months after fledging (Balotari-Chiebao et al., 2021), with certain individuals staying even longer (Hardey et al., 2006). Therefore, the first 100 days of tracking for each individual was removed from the dataset in this analysis, avoiding the territorial attachment to the nest during this phase. In addition, nesting adults were also excluded from the analysis due to their territorial attachments. Thus, only the wide-ranging and non-territorial sub-adults between 1-4 years were included. The raw data also showed that certain individuals died or experienced disturbances in the GPS-tracking shortly after fledging, mostly within the range of 50-200 days. This is opposed to most of the individuals, for which the tracking ranged over several years. Therefore, individuals with less than 100 days of tracking and 500 relocations in total was removed, as these limited sample sizes may cause inaccurate home range estimations. The final count of actual relocations used for the analysis was 250 799 distributed among 34 individuals. The total relocation counts for each individual ranged from 631 to 43 799, with most individuals ranging between 1 000 - 10 000 relocations.

2.3.2 Home range estimation

The home ranges for each individual eagle ID were estimated using the Brownian Bridge Movement Model (BBMM). The BBMM is a favorable approach in animal home range analyses as the estimations are based on the animal's trajectories and considers the time elapsed between different relocations (Buchin et al., 2015). Is this way, the BBMM copes with issues related to temporal autocorrelation, which can occur in standard utilization distribution methods with the assumption of dependent observations. The BBMM assumes that the movement pattern between two consecutive locations is random (i.e. brownian), thus limiting the uncertainties related to irregular GPS-fixes (Buchin et al., 2015; Fischer et al., 2013). The home range estimations were conducted as an initial step of the resource selection modelling process, which is described in chapter 2.4. 34 different home-range polygons were created using the "kernelbb" function from the "adehabitatHR" package (Calenge & Fortmann-Roe, 2023) in RStudio version 2023.12.1 (RStudio, 2015) (see Appendix B). This version of RStudio was used for all programming tasks in this thesis.

2.4 Resource selection modelling

A resource selection model was developed to obtain information of the habitat preferences of the white-tailed eagles. A total number of 539 250 locations were analyzed, of which 288 451 were random points (ca. 1.15 x actual relocations). These random points are called pseudo-absences and represent the areas that could be utilized within the home range of each eagle (i.e. the available habitat) (Barbet-Massin et al., 2012). A generalized linear mixed-effects model (GLMM) was fitted to the data using the "glmer" function from the "lme4" package (Bates et al., 2015). The response variable in the model was set as binomial, representing the presence (actual observation = 1) or absence (random point = 0) of eagles at a given point. Logistic regression was utilized to model these outcomes, providing a probabilistic framework suitable for predicting eagle occurrences based on spatial and environmental variables. The fixed predictor variables were categorical variables that included different aggregated land cover types (see Appendix A), and continuous variables that included elevation above sea level, slope level (in degrees), topographic position index (TPI) and distance to shoreline. Individual eagle IDs were set as random effect to cope with the non-independence and possible intra-class correlation of the data (Bolker et al., 2008).

The full resource selection model containing all variables was examined using the "dredge" function from the "MuMIn" package (Bartoń, 2023). This process breaks up the model and test all possible variable combinations, ranking the models by using the ΔAIC, with models with ΔAIC < 2.0 considered as best (Burnham & Anderson, 2004). In some cases, the data of two or more predictive variables can have a linear relationship and explain the same type of variation. This is known as collinearity and may cause biased and non-representative models if not addressed (Hendrickx & Utrecht, 2018). The collinearity between the continuous predictive variables were analyzed using the Variance Inflation Factor (VIF) provided by the "car" package (Fox & Weisberg, 2019). The VIF explains the extent of the linear relationships between the predictor variables (Forthofer et al., 2007). In the global model "distance to shoreline" had some level of collinearity with the elevation variable, and distance to shoreline were not included the final model.

The best model showing the predicted probabilities of eagle presence in all habitat categories was graphically presented using the "ggpredict" function from the "ggeffects" package (Lüdecke, 2018). A preference or avoidance of a particular habitat was inferred if the predictions were notably above or below the 50 percent expectation. Conversely, no preference or avoidance was inferred if the

confidence intervals of the predictions overlapped with the 50 percent mark. This indicates that the observed habitat use aligns with what would be expected by chance, signifying no significant deviation from random distribution. In the model, agricultural areas are set as the baseline against which other habitat categories are compared. The model automatically selects agricultural areas as the baseline because they come first alphabetically. Given that the initial model results inherently depend on the choice of the baseline, and to thoroughly understand the relative preferences or avoidances across all habitat categories, a post-hoc analysis was conducted. This analysis involved pairwise comparisons between the predicted probabilities of eagle presence in each habitat category. This was done by seeing whether the confidence interval of one category overlapped with the confidence interval of another after graphically presenting the best model. If no overlap was observed, the probability of the categories was significantly different from each other, and vice versa.

The elevation variable explains the eagles' elevation preferences, were a positive or negative value indicates whether eagle presence increases or diminishes with increasing altitude. The same concept applies for the slope variable with increasing steepness in the terrain. Lastly, a positive or negative value for the TPI variable indicates whether eagle presence is more likely on hilltops or in valleys, respectively.

2.5 Flight risk modelling

A logistic GLMM was also fitted to the flight altitudes to map out the areas where the eagles are flying at risk heights. The flight altitudes for each relocation were obtained by subtracting the altitude from the transmitter with the registered elevation level from the digital terrain model (DTM). The response variable was set to whether the eagles were flying at risk heights vs. flying at non-risk heights in relation to onshore wind turbines. The eagles were defined as "in flight" with an instantaneous speed at $\geq$ 1 km/h at the time of registration (May et al., 2011). Moreover, some individuals may have been soaring against strong wind currents, measuring no speed even though they are in flight. Therefore, the eagles were also determined as in flight at speeds < 1 km/h at altitudes above 50 meters. The altitude limit was set to avoid the possibility of individuals roosting or perching in trees.

The optimal flying altitudes associated with increased collision risk were found by using the average measurements of existing wind turbines in Norway. The tower height of most commercially operative Norwegian wind turbines are between 80 – 145 meters, while the rotor blade diameter stretches between 60 – 80 meters (NVE, 2024a). Thus, the radius of the rotor blade diameter can be added and subtracted from the tower heights for the smallest and largest turbines. This will result in the maximum and minimum altitudes of the rotor swept zones (RSZ), respectively. As a results, based on the average measurement Norwegian wind turbines, the eagles were determined to fly at risk altitudes between 50 – 185 meters. Observations that fell within this range of risky altitudes were registered with response = 1, while those flying above or below were registered with response = 0.

For this model, the predictor variables used was similar to those in the full resource selection model. "Distance to shoreline" was again excluded due to collinearity with the elevation variable. However, a fourth continuous variable showing the ruggedness of the terrain was also included in the global flight risk model but was excluded due to collinearity with the slope variable. To evaluate habitat associations with risk, post-hoc pairwise comparisons were again conducted to assess differences in probabilities of flying at risk heights, based on whether confidence intervals overlapped in the model outputs. For elevation and slope, positive or negative estimates suggest that the predicted probabilities of an eagle flying at risk heights increases or decreases as the elevation and terrain steepness increases. Lastly, for the TPI, a positive estimate suggest that eagles are more likely to fly at risk heights at hilltops. With a negative estimate, the same applies for valleys.

2.6 Collision risk model

The final model used to calculate the total landscape-based risk was a collision risk model based on the mathematical approach used in Tucker (1996). The model calculated the predicted probabilities of direct turbine collision across the landscape based on the following technical, biological, and environmental parameters:

- Turbine data: Height, number of rotors blades, rotor blade length, pitch, axial induction factor and max chord.
- Gears: List of wind speeds with corresponding turbine gears.
- Bird data: Average flight speed and flight direction (angle of approach in degrees).

- Bird shape: Wingspan and length.
- Wind data: Nationwide wind speed raster map, with each pixel containing an average wind speed at 80 meters above sea level.

The collision risk is calculated by comparing the time the eagles uses to fly through the rotor swept zone (RSZ), and the time is takes the rotor blades to complete one full circular motion (Masden & Cook, 2016; Tucker, 1996). The turbine data and gears are based on the average measures and mechanics of Norwegian wind turbines, while the wind data were obtained from a nationwide wind speed map at 80 meters above ground level. The bird data were gathered from the extensive GPS-dataset from NINA. By incorporating all parameters, the collision risk was calculated across the landscape as a function of the angle of approach, ranging from -180 to 180 degrees. This allowed the model to account for each possible flight direction relative to the wind turbines, thereby achieving a collision risk factor for each possible angle. This is important, as the probabilities of collision is highly influenced by the flight angle in relation to the turbine (Holmstroma et al., 2011). The model also accounted for all possible wind speed directions. Lastly, the average predicted collision probability was calculated for all the different wind speeds across the landscape (Tucker, 1996). The visual presentation of the collision risk model is shown in chapter 3.3.3.

2.7 Predictive risk mapping

The best models for resource selection and flight altitude were graphically presented using the "raster" package (Hijmans, 2023) in RStudio. Creating predictions of animal distributions and other factors across the landscape is an important tool in biodiversity conservation strategies (Morris et al., 2016). It has also been previously used in understanding the effects of human activity on different animal species and their ecology (Hebblewhite & Merrill, 2008; Merkle et al., 2011). In this study, each raster layer used for data sampling in the model prediction was used to create a joint data frame of pixels. A crucial part was making sure that all the input layers had the exact same dimensions and extent, and the layer names matched the names of the predictor variables in the best predictive models. Furthermore, predictive maps were created by combining the results of the best models with the data frame. By using the integrated R-function "predict", each pixel was given a value of predicted eagle presence and probability of flying at risk height based on all predictor variables. These results were extrapolated to the entire study area (central and northern Norway), creating two separate maps

showing areas of high to low probability of presence and probability of flying at risky flight altitudes. The dimensions used for the resource selection and flight risk maps was 17 203 X by 20 850 Y, and despite the wide-ranging outreach, the maps were highly detailed with a pixel size of 50 x 50 meters. This means that each pixel covers an area of only 50 meters in length and width. The total pixel count for the maps was 358 682 550, given the dimensions.

The direct collision risk model was graphically presented by running the model on each separate pixel in the wind speed raster map. In this way, the model used all input parameters mentioned in chapter 2.6, and a different wind speed given the value in each pixel. This resulted in a large scale collision risk map with each pixel representing the collision risk factor as an average of every angle of approach. Furthermore, the collision risk map was multiplied with two previous predictive maps. This process combined the existing risk levels based on environmental variables, and the turbine collision risk levels across the landscape by multiplying each raster pixel with each other. The collision risk map had a large pixel size of 2415 x 2415 meters due to the original scale of the input wind speed map. Hence, the collision risk map was resampled to match the dimensions and pixel size of the two previous predictive maps before multiplication could take place. For this process, the "resample" function from the "raster" package was used (Hijmans, 2023). The multiplication of the three separate predictive maps resulted in a new final map showing the distribution of the total predicted collision risk across the landscape based on all model results (i.e. the eagles' landscape of risk). The map shares the scale and resolution of the resource selection and flight risk maps and is presented in chapter 3.3.4.

2.8 Collision risk by existing wind farms

The collision risk levels for each existing wind farm within the study area was assessed in two different ways. In the first approach, the map representing the eagles' landscape of risk was overlayed with the locations of existing wind turbines in QGIS. The total risk values were extracted for each turbine in the study area using the QGIS algorithm "sample raster values" and summed across the existing wind farms. The risk levels for each wind farm were then presented as risk per megawatt installed capacity. The second approach was more comprehensive, and utilized the existing link between resource selection and population density (Bourgeron et al., 1999). Here, the total risk per wind farm was calculated as a proportion (in percentages) of the total population across the study area

which is expected to collide at any given point in time. This was done by changing the predicted presence map by dividing the presence value in each pixel with the sum of probabilities across all pixels in the map. In this way, the presence probabilities in each pixel were normalized into values representing a proportion of the entire population across the study area, where the sum of predicted presence across all pixels amounted to 1 (i.e. 100 %). The normalized presence probabilities were multiplied by the flight risk map and the direct collision risk map like the process described in chapter 2.7. This resulted in a new collision risk map, in which each pixel represented a proportion of the total population across study area that are expected to collide at any given point in time. These values were extracted for each turbine in the study area and summed across the existing wind farms.

2.9 Cumulative collision risk per individual

The cumulative collision risk for each individual eagle in the analysis was calculated by using the eagle's movements trajectories from the BBMM. The trajectories were used to map the areas where the movement patterns intersected with existing wind farm sites. This method has previously been used in the assessment of flight path changes of large-bodied birds in relation to onshore wind farm constructions (Therkildsen et al., 2021). Next, the number of different wind farms intersected for each eagle were counted, as well as the total amount of wind farm intersections for each eagle. Lastly, the collision risk levels for the intersected wind farms were summed across the individual movement trajectories, resulting in the cumulative risk of collision for each individual. Here, the average collision risk per turbine was used by dividing the total risk per wind farm with the number of turbines. The total risk per wind farm was obtained from the final collision risk map presented in chapter 3.3.4.

3. Results

3.1 Resource selection modelling

The best (most parsimonious) predictive resource selection model based on the ΔAIC showed clear differences in the habitat preferences of the eagles. This model included all categorical and continuous variables, except "distance to shoreline". The parameter estimates are presented in Table 1. The eagles mainly preferred open and sparsely vegetated areas. The probability of a given point being an actual

Table 1: Parameter estimates from the best fitted model. Logistic regression with eagle observations vs random points as function of the different categorical and continuous predictive variables (agriculture as intercept).

Fixed effects	**Estimate**	**Std. error**	**P-value**
Intercept	-0.720	0.110	< 0.001 ***
Bare rock / Scarce vegetation	1.048	0.018	< 0.001 ***
Forests	-0.353	0.020	< 0.001 ***
Inland waters	-0.432	0.047	< 0.001 ***
Marine waters	-0.708	0.016	< 0.001 ***
Shrubland	1.126	0.021	< 0.001 ***
Urban	-1.957	0.074	< 0.001 ***
Wetlands	0.920	0.019	< 0.001 ***
Elevation	-1.472	0.009	< 0.001 ***
Slope	0.762	0.006	< 0.001 ***
TPI	0.247	0.004	< 0.001 ***

eagle relocation is higher in shrublands, and areas associated with bare rock and scarce vegetation, compared to the expectation (Fig. 2). The probability of eagle presence in wetlands was also marginally higher than the expectation, indicating a slight selection preference. However, the confidence interval overlaps with the 50 percent threshold line, suggesting that the preference is not statistically significant and not significantly different from chance (Fig. 2). In contrast, eagles avoided urban areas and human infrastructure. The predicted probability of eagle presence in the urban habitat category is located well below the expectation, meaning that eagles use the urban category significantly less than the availability (avoidance). This result is also supported by the small and non-overlapping confidence interval. The predicted probability of eagle presence in agricultural areas was also significantly less than the expectation, yet still substantially higher than in urban areas. The eagles also used the forests and both water categories significantly less than the availability (Fig. 2). Moreover, there was significant differences in predicted probabilities between all the categories above the threshold line (including wetland) and those below, due to the non-overlapping confidence intervals (Fig. 2). There were also significant differences between agriculture, marine waters, and urban areas. The urban habitat category also remained the only category significantly different from all other categories.

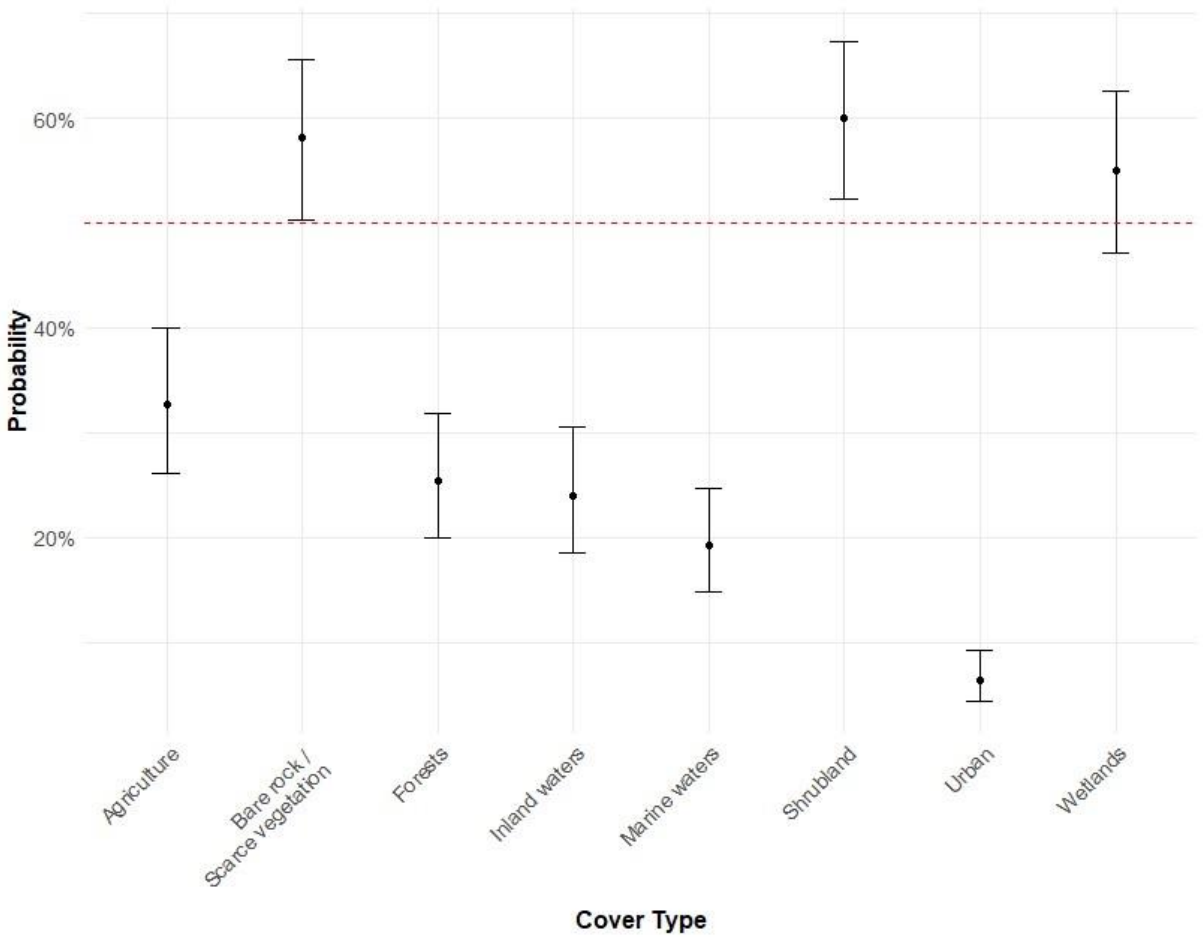

Figure 2: Predicted probabilities of eagle presence (response = 1), with 95 % confidence intervals, at different aggregated habitat categories. The red line represents the expectation at 50 percent. Predicted probabilities above or below the line indicates a selection towards and against the habitat category, respectively.

The negative estimate for elevation shows a clear selection towards flat and more uniform areas, and avoidance of mountainous areas and areas of substantial topographic variation (Table 1). The probability of eagle presence is decreased with increasing altitude, meaning that eagle presence becomes less likely as the altitude above sea level increases (Fig. 3). The opposite was observed for slope, as the predicted probability of eagle presence increased with increasing degree of slope in the landscape. The eagles also selected areas with a positive TPI, meaning that hilltops were more favorable than valley-shaped areas (Fig. 3). The visual presentation of the best resource selection model is shown in chapter 3.3.1.

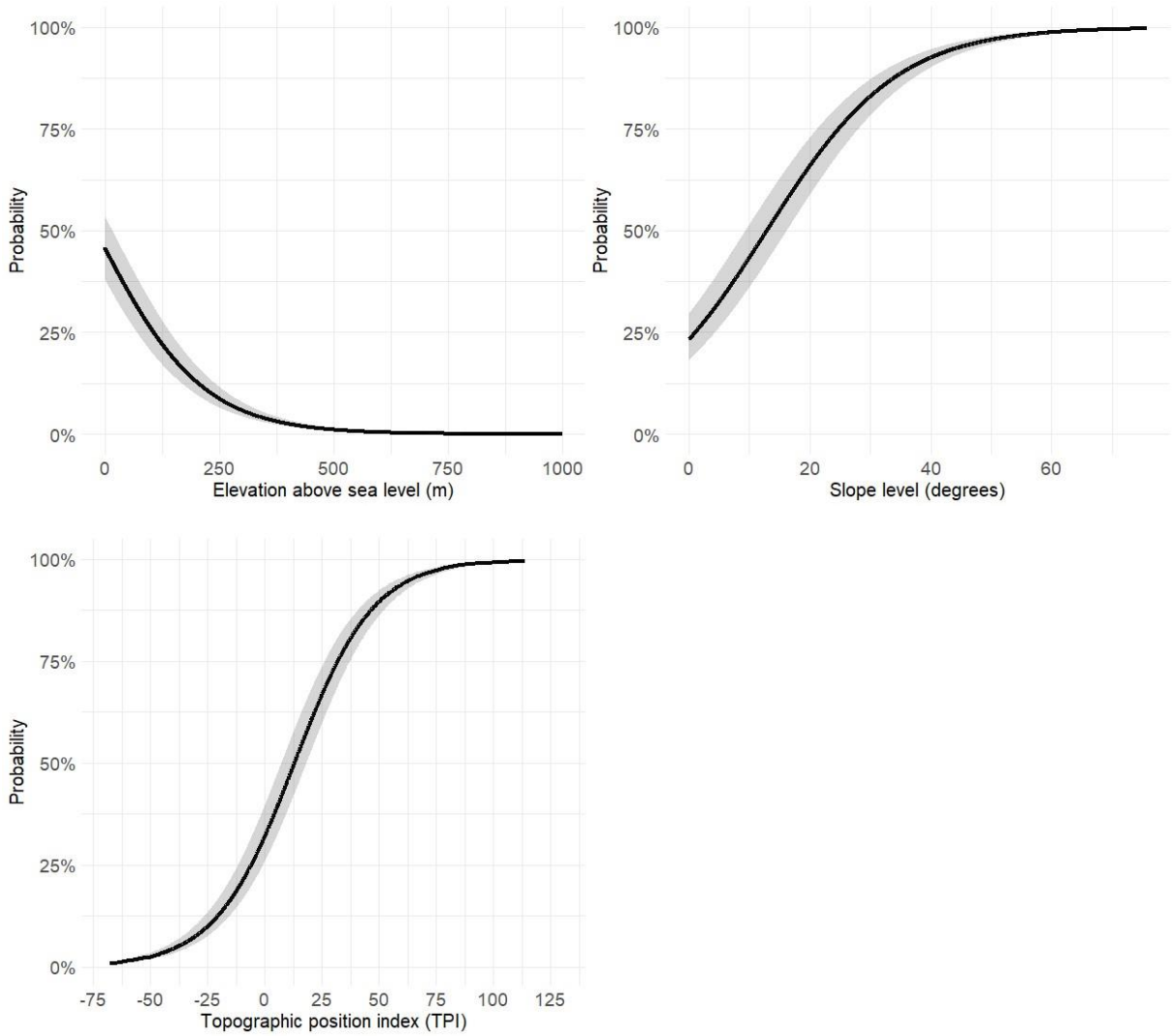

Figure 3: Predicted probabilities of eagle presence (response = 1), with 95 % confidence intervals, as function of elevation above sea level, terrain steepness and topographic position index.

3.2 Flight risk modelling

The best model estimating the predicted probabilities of eagles flying at risk heights included the same predictor variables as the best resource selection model, with distance to shoreline and terrain ruggedness being excluded. The parameter estimates for the categorical and continuous variables are presented in Table 2.

Table 2: Parameter estimates from the best fitted flight risk model. Logistic regression with flying at risk heights (50 – 185 m) vs flying below or above as function of the different categorical and continuous predictive variables (agriculture as intercept).

Fixed effects	**Estimate**	**Std. error**	**P-value**
Intercept	-0.736	0.087	< 0.001 ***
Bare rock / Scarce vegetation	-0.283	0.058	< 0.001 ***
Forests	0.266	0.062	< 0.001 ***
Inland waters	0.411	0.126	0.0011 **
Marine waters	-0.262	0.058	< 0.001 ***
Shrubland	-0.165	0.066	0.0120 *
Urban	-0.013	0.374	0.9724
Wetlands	-0.035	0.062	0.5709
Elevation	0.106	0.013	< 0.001 ***
Slope	0.336	0.014	< 0.001 ***
TPI	-0.230	0.011	< 0.001 ***

The highest probabilities of flying at risk heights were observed over forests and inland waters, which were significantly higher than those observed over bare rock / scarce vegetation, shrubland, marine waters, and wetlands (Fig. 4). The eagles were least likely to fly at risk heights over bare rock/scarce vegetation, shrublands, and marine waters. The confidence intervals for these cover types were also relatively narrow, indicating accurate predictions. Moreover, the probability of flying at risk heights in shrublands was nearly the same as over marine waters and bare rock / scarce vegetation. In comparison, the risk was slightly higher when flying over agricultural areas and wetlands. Flying over urban areas was, on average, associated with a risk similar to that of agriculture, although these predictions came with considerable uncertainty due to the wide confidence intervals (Fig. 4).

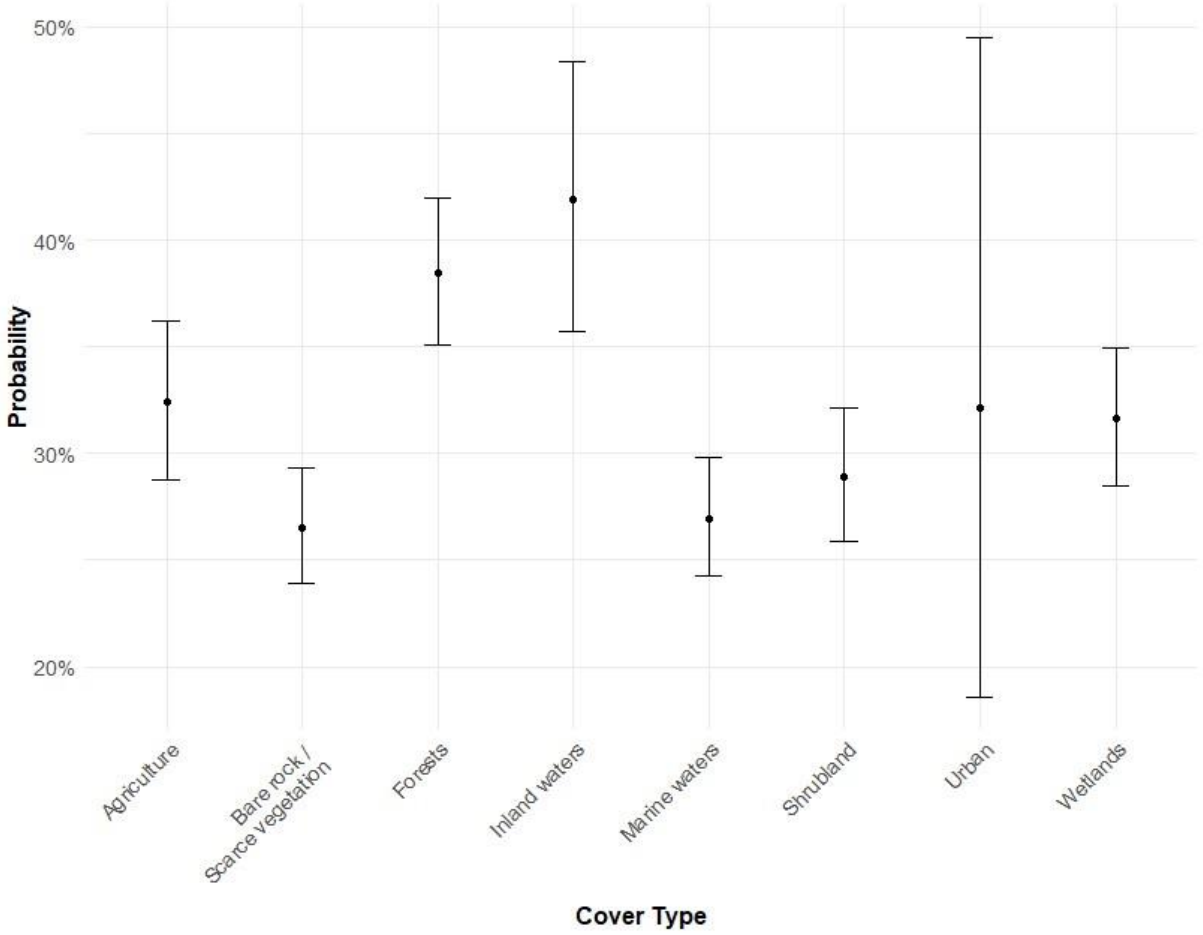

Figure 4: Predicted probabilities of eagles flying as risk heights (response = 1), with 95 % confidence intervals at different aggregated habitat types. Overlapping confidence intervals suggest that the probability in these categories is not significantly different from each other.

For the continuous variables, the predicted probability of an eagle flying at risk height was increased with increasing elevation above sea level and terrain steepness (Fig. 5). In other words, the eagles were more likely to fly at risk heights in mountainous areas and in areas characterized by steep slopes. The predicted probability was decreased with increasing TPI, suggesting that eagles were more likely to fly at risk heights in valleys than on hilltops (Fig. 5). The visual representation of the best flight risk model is shown in chapter 3.3.2.

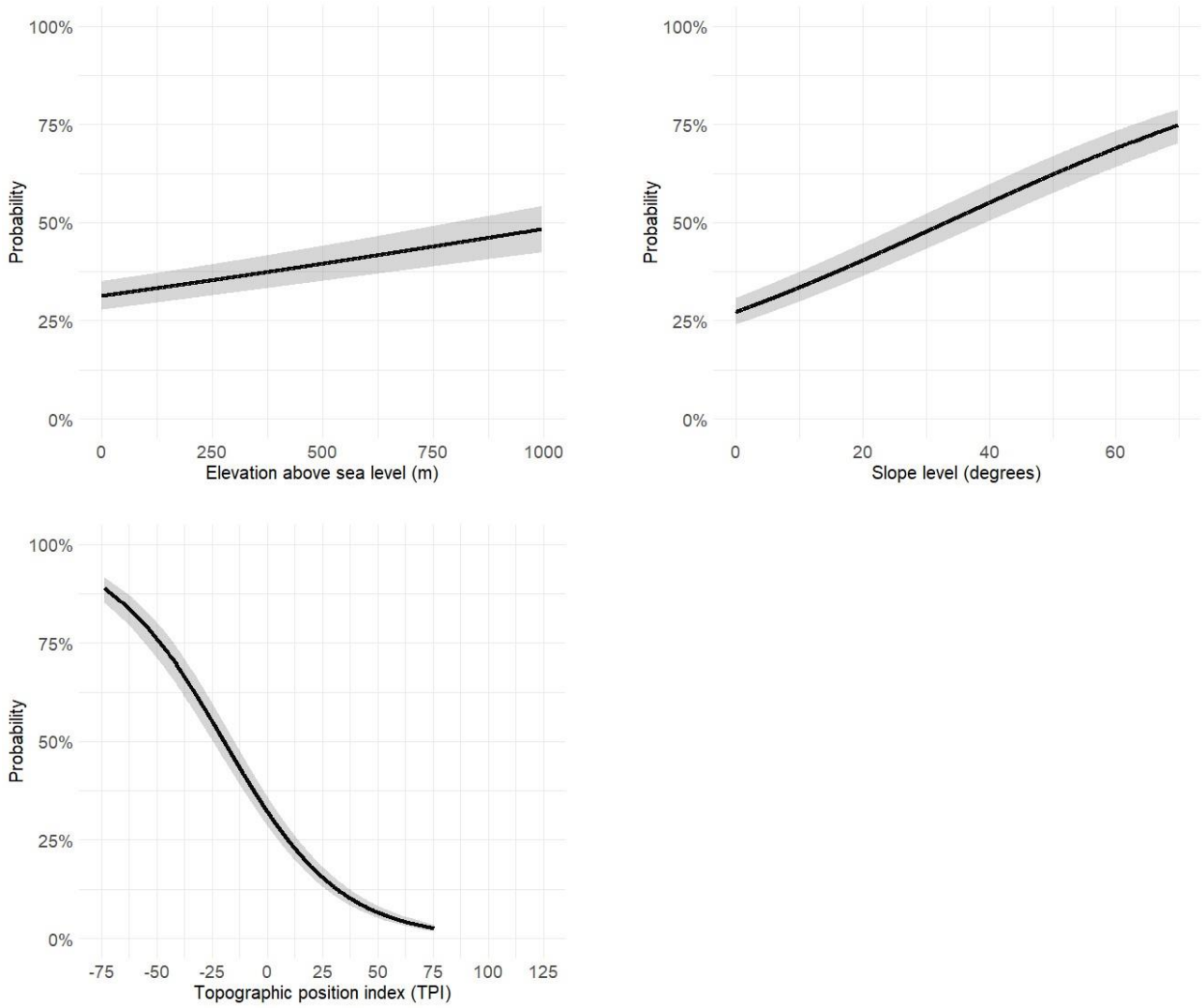

Figure 5: Predicted probabilities of an eagle flying at risk heights (response = 1), with 95 % confidence intervals, as function of elevation above sea level, terrain steepness and topographic position index (TPI).

3.3 Predictive maps

3.3.1 Resource selection model

The visual presentation of the resource selection model shows the distinctive preferences towards sparsely vegetated coastal habitats and represent a gradient from coastal to inland landscapes. The probability levels are presented on a continuous scale due to the wide range of data in the model results. This allowed the variability in the data to be well presented with equally large ranges (Fig. 6).

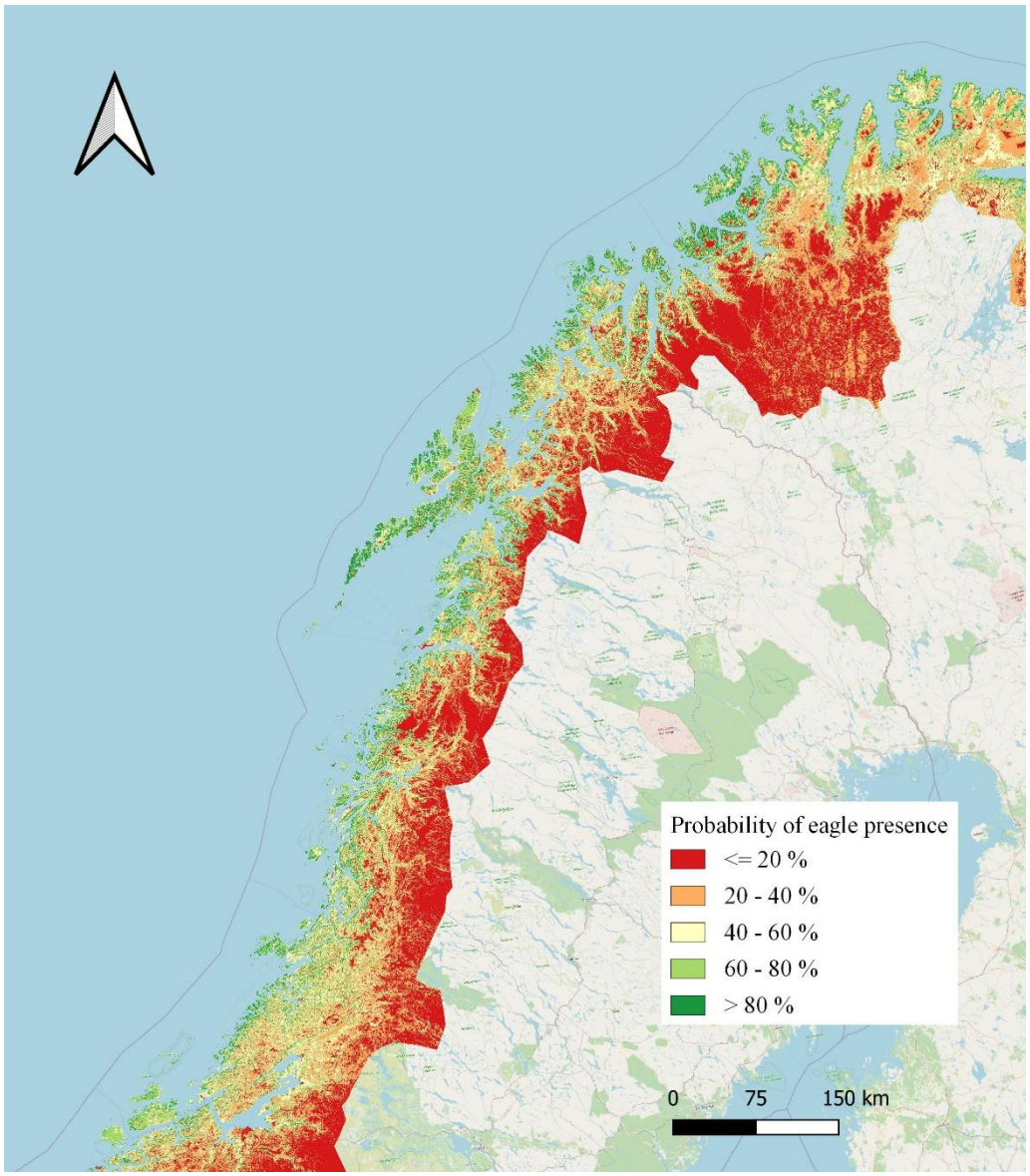

Figure 6: Visual presentation of the best resource selection model, covering the northern movement patterns of the all the individuals included in the model. The color-range is shown at a continuous scale from red to green, indicating low to high preference, respectively.

3.3.2 Flight risk model

The visual representation of the flight risk model clearly depicts that the environmental variables increasing the risk of flying at risk heights are mostly very different from those increasing eagle presence in general (Fig. 7). The variation in the probability levels is also relatively low compared to the resource selection map. Therefore, the data is presented at a quantile scale, where each data range contains the same number of values. This helps to visually highlight the differences better within less variable data.

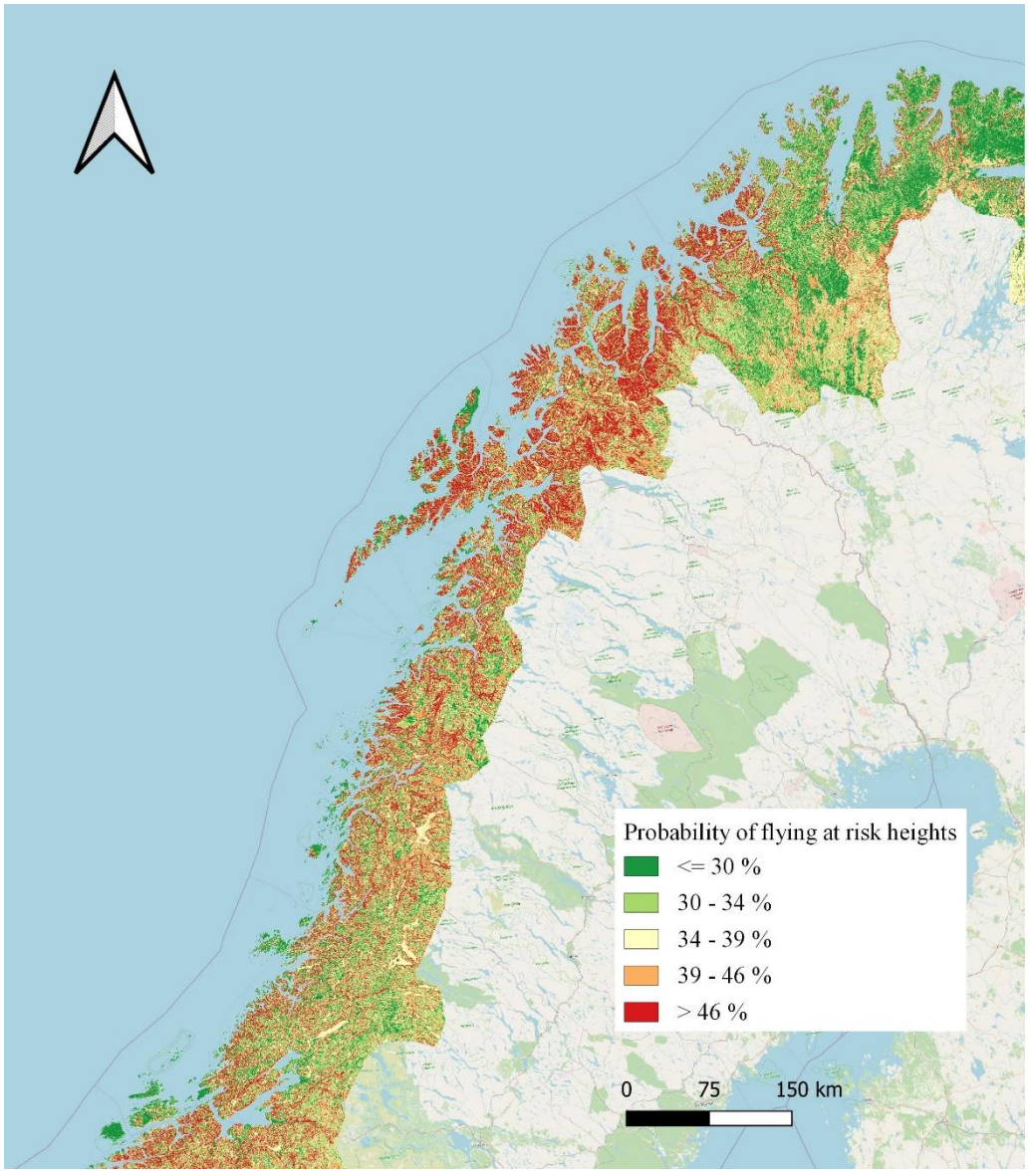

Figure 7: Visual presentation of the best model of the predicted probabilities of white-tailed eagles flying at risk heights. The color-range is presented as quantiles from green to red, indicating low to high probability, respectively.

3.3.3 Collision risk model

The collision risk model suggests that the risk of colliding with a wind turbine is evenly distributed across the landscape (Fig. 8). The general variability in risk levels is also relatively low, only ranging from about 20 to 30 % mostly due to the changes in average speeds from pixel to pixel. Thus, the data are presented in quantile scale like the flight risk model.

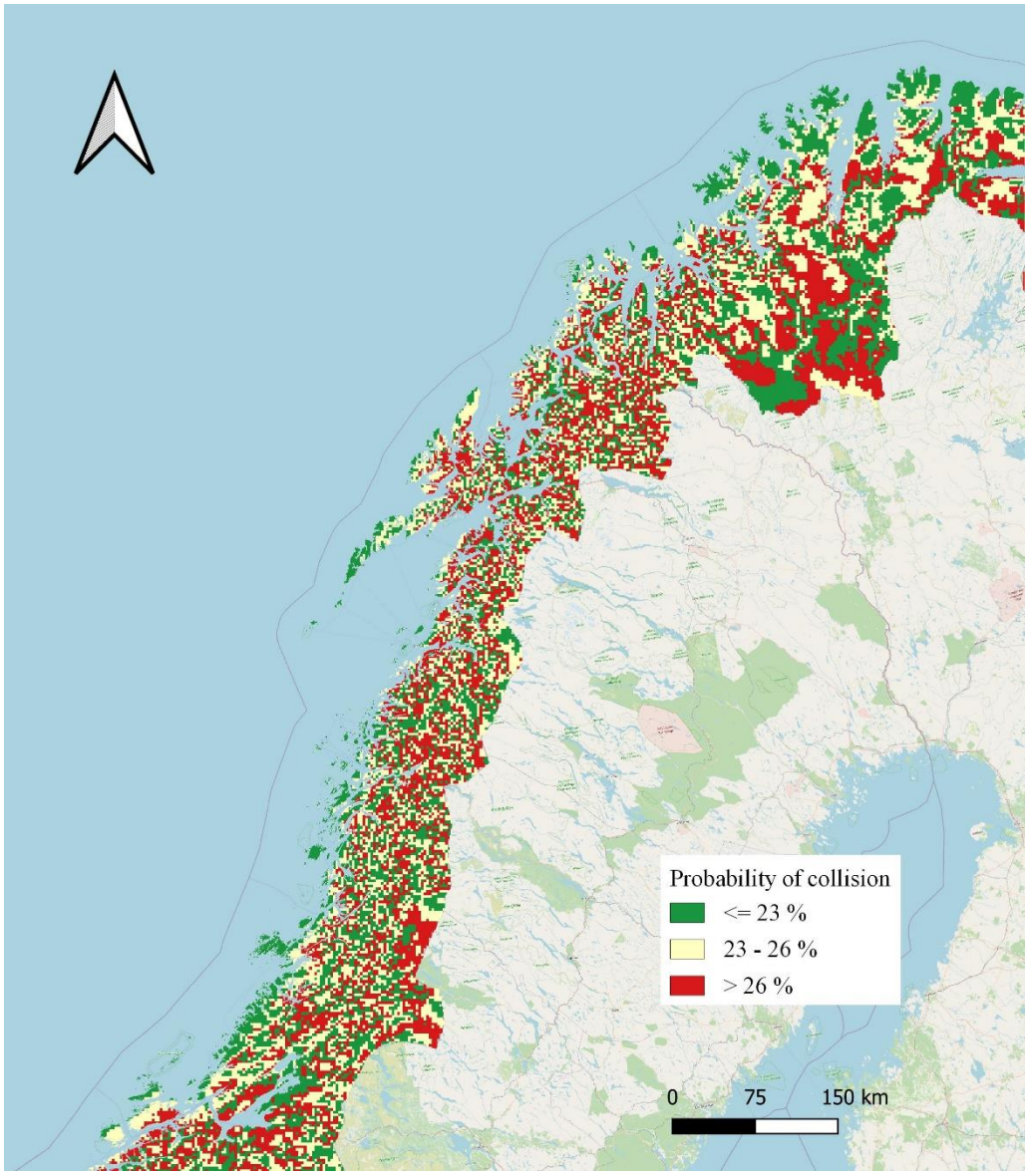

Figure 8: Visual presentation of the direct collision risk model, given all technical, environmental, and biological input parameters. The color-range is presented as quantiles from green to red, indicating low to high probability, respectively

3.3.4 Combined landscape of risk

By multiplying the predictive values in all the three previous maps combined, the total collision risk based on all environmental, biological, and technical parameters was visually presented across the landscape. Unsurprisingly, the total collision risk was strongly correlated with the predicted probability of eagle presence and increased towards coastal lowland regions (Fig. 9). This is caused by the higher probability values in the resource selection map, which have a substantial effect on the total collision risk. This is particularly evident in the areas around the fjords, which is characterized by steep terrain. The map is presented at a quantile scale, equal the previous maps.

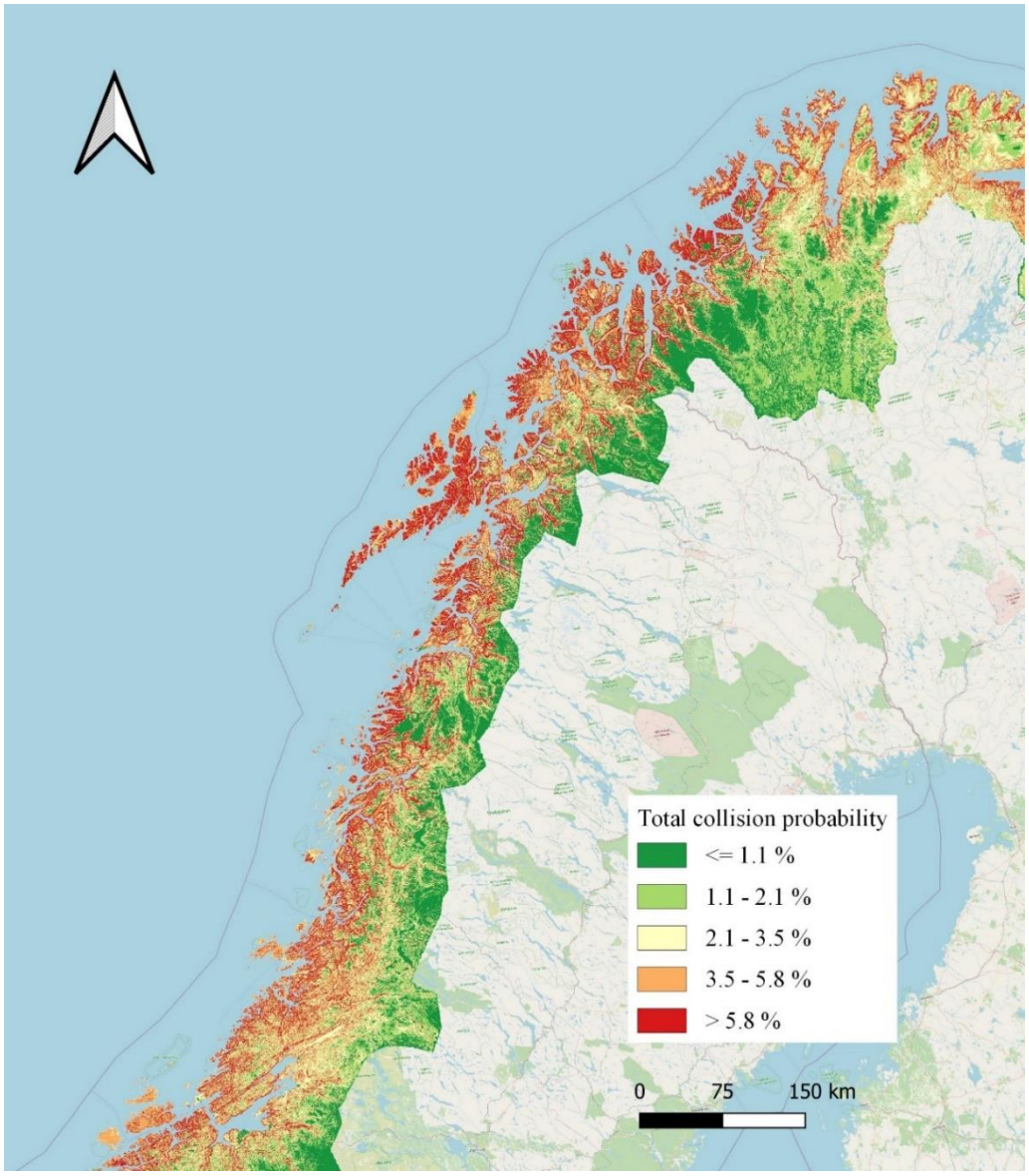

Figure 9: Visual presentation of the eagles' predicted landscape of risk as percentages, based on the model results of the resource selection, flight risk and direct collision risk. The color-range is presented as quantiles from green to red, indicating lower to higher probability, respectively.

3.4 Collision risk by existing wind farms

Here, the risk levels for each wind farm are first presented as the proportion of the total population across the study area that are expected to collide at any given point in time (Fig. 10). Note that the overall low proportion levels per wind farm is linked to the immense scale and resolution of the resource selection map. Each pixel represents a proportion of the total population across the entire study area, which amounts to 100 % when summed across all pixels. There was great variation in the predicted risk levels, with most high-risk wind farms being in the southern part of the study area. It is worth noting that wind farms with a high number of turbines usually have higher total collision risk, even though some smaller wind farms might have a higher average risk. The greatest predicted

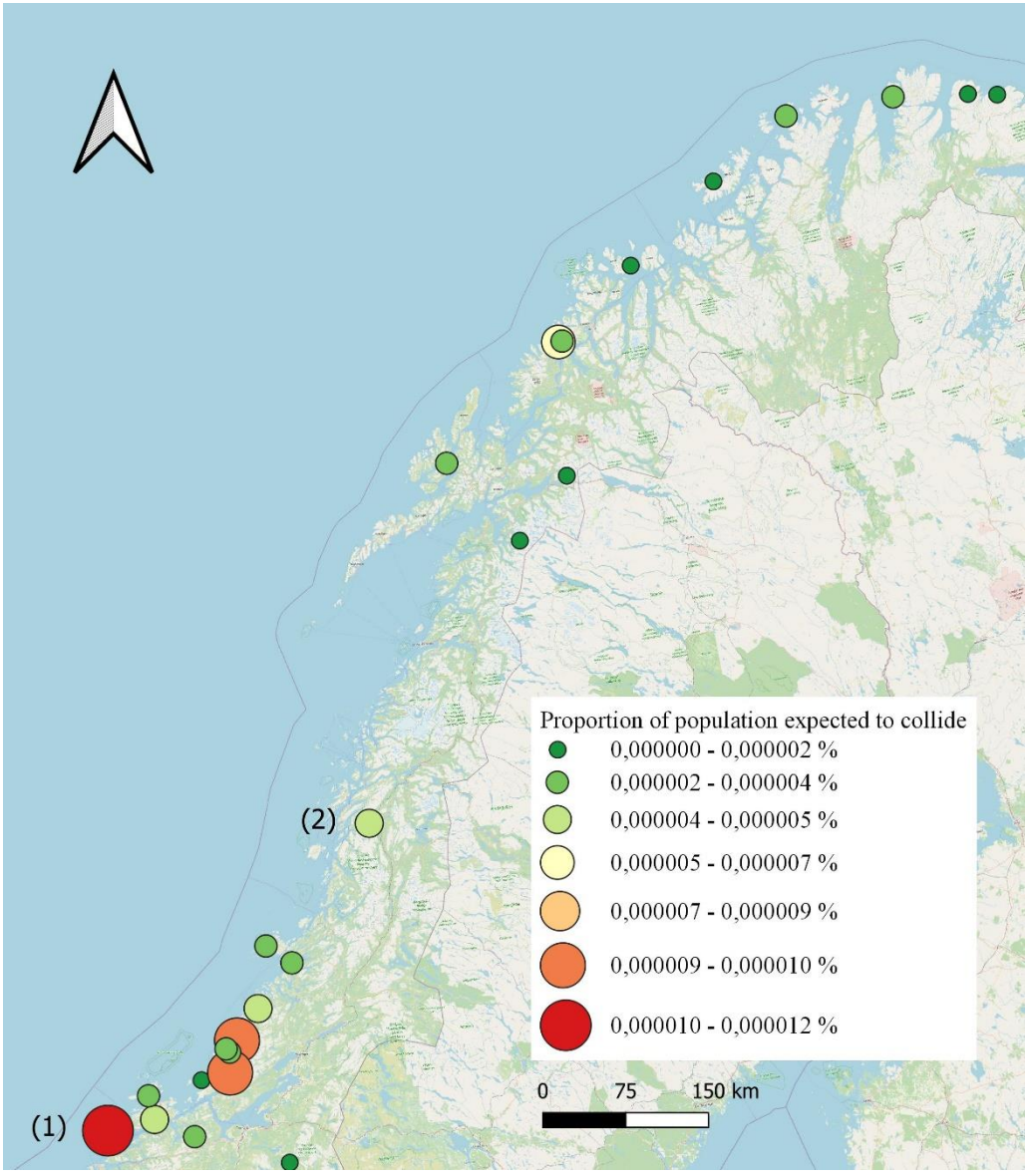

Figure 10: Visual presentation of the total risk posed by existing wind farms within the study area. The risk levels represent the proportion of the total population across the study area that are expected to collide at any given point in time.

risk is found at Smøla wind farm (1). It consists of 68 turbines, all of which with a relatively high collision risk, resulting in a high wind farm scaled risk. This differs from other wind farms of equal magnitude, such as Øyfjellet wind farm (2). Based on the model results, most of the 72 turbines have little to no predicted risk, resulting in a significantly lower total collision risk (Fig. 10). Further north, the general predicted risk of collision among the wind farms is low. However, the collision risk across several wind farms drastically changes when the risk levels were presented per megawatt installed capacity (Fig. 11). Some of the smaller wind farms with a low total collision risk have a higher collision risk relative to its size. On the other hand, some of the larger wind farms with a high total collision risk had a considerably lower risk compared to its size and production contribution.

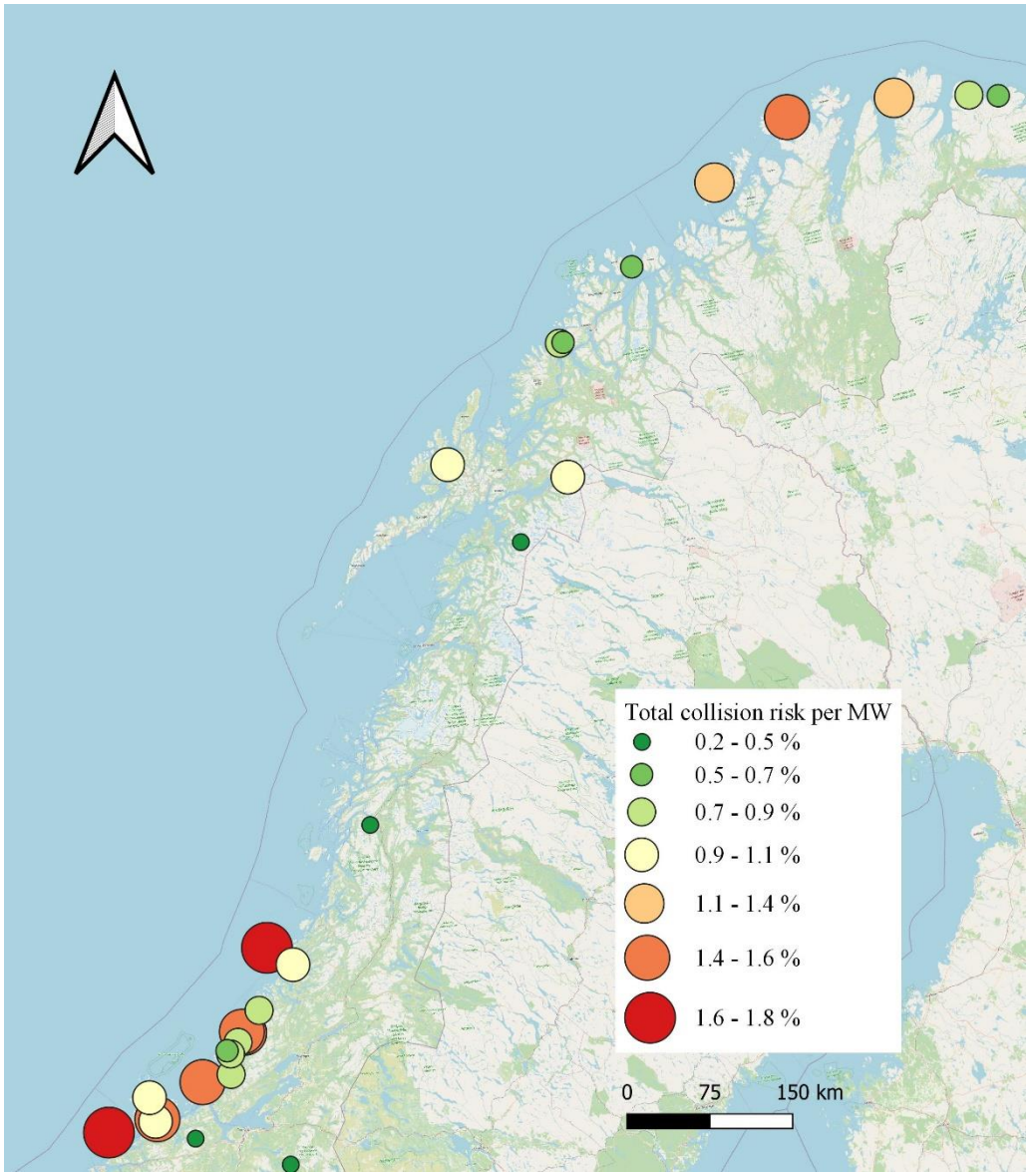

Figure 11: Visual presentation of the total collision risk per wind farm, shown as total risk per megawatt (MW) installed capacity.

3.5 Cumulative collision risk per individual

In the cumulative risk assessment, the movement trajectories showed that all the eagles included in the analysis moved through at least one wind farm throughout the tracking periods (Fig. 12). However, there was a relatively high level of variation among individuals. Nine individuals moved through ten or more different wind farms, while six individuals flew through three or less. The average number of unique wind farms intersected per eagle was 6.62. Most of the northern movements took place in the spring and decreased during the summer.

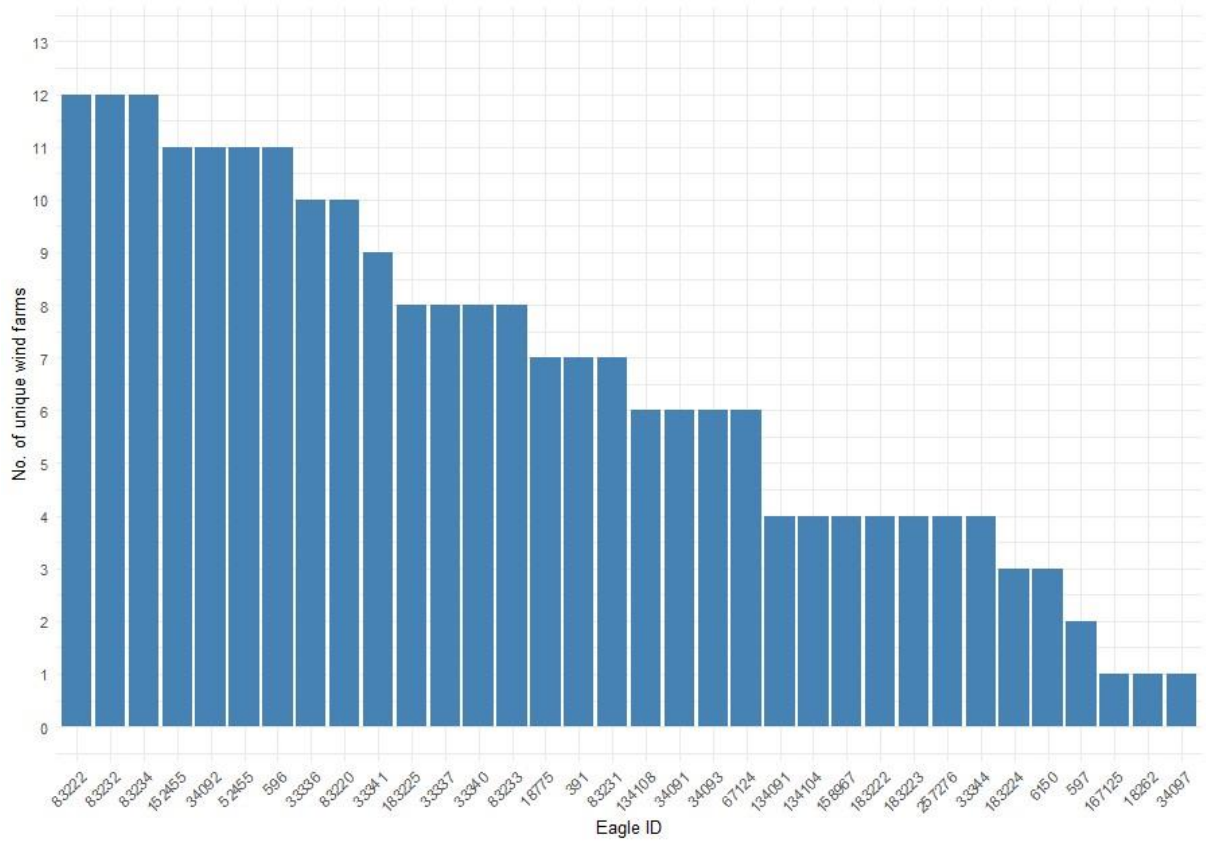

Figure 12: The number of different wind farms intersected per individual.

The total number of wind farm intersections was also higher than the number of unique wind farms intersected for most individuals (Fig. 13). This suggests that most eagles intersected at least one wind farm more than once, increasing the cumulative risk of collision. For instance, ID 83231 intersected seven unique wind farms through the tracking period but had a total of 12 intersections in total.

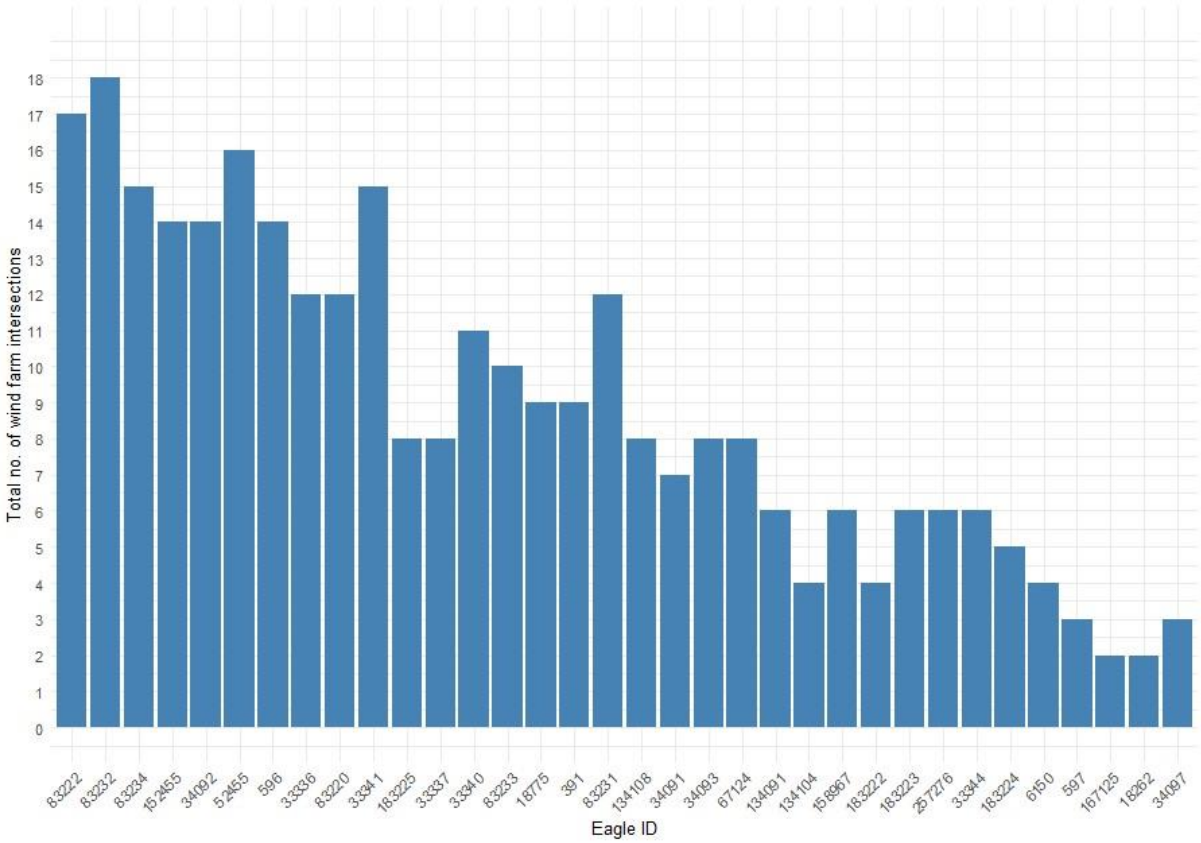

Figure 13: The number of wind farm intersections in total, independent of unique wind farms. The order of eagle IDs on the x-axis is equal to figure 12.

Based on the collision risk levels of each wind farm and the total numbers of wind farms intersected, the eagles were facing different levels of cumulative collision risk along their movement paths (Fig. 14). Unsurprisingly, the cumulative collision risk is strongly correlated with the number of intersected wind farms. However, there were some notable differences where certain individuals faced a lower cumulative collision risk despite intersecting the same number of unique wind farms and intersections in total. This suggests that some individuals avoided the high-risk wind farms more effectively. ID 33337 and 183225 was two of the least risk exposed individuals relative to the number of different wind farms intersected (8). On the other hand, ID 33340 intersected the same amount of different wind farms but moved through at least one wind farm more than once during the tracking period. This resulted in a substantially higher cumulative risk.

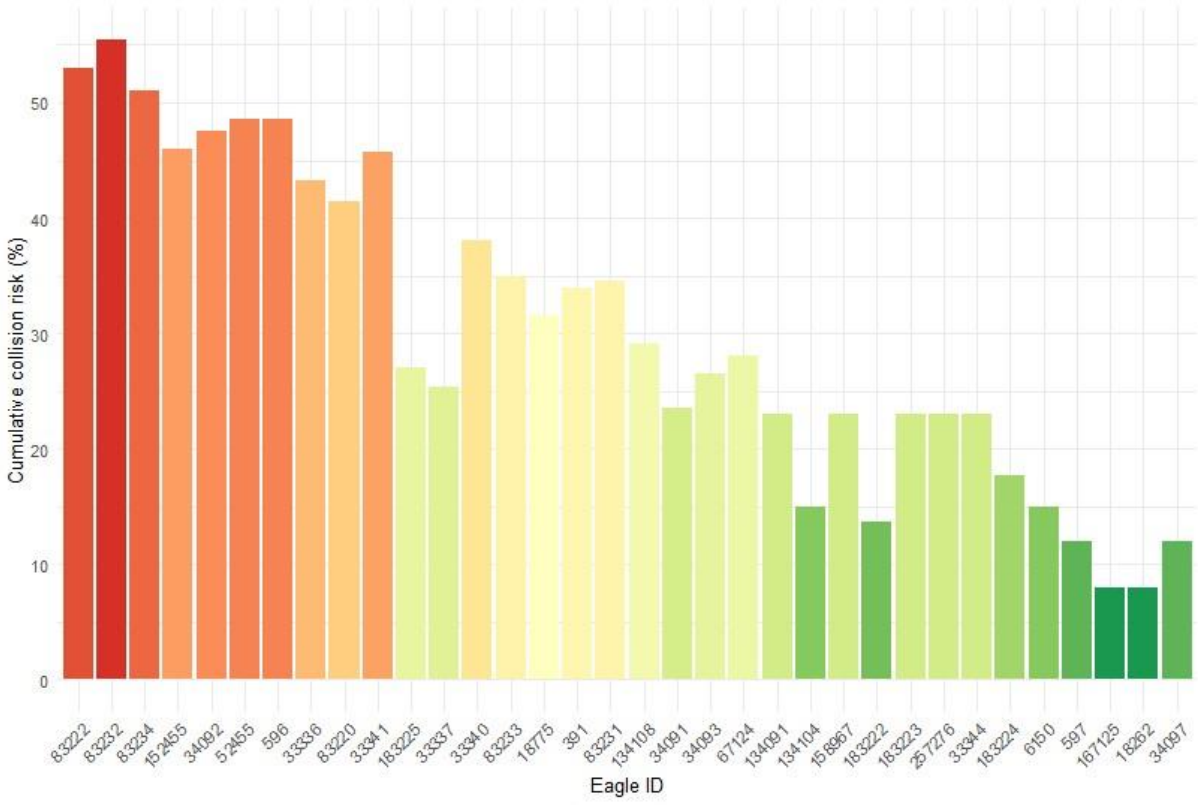

Figure 14: Cumulative risk of collision for each eagle along their movement trajectories. The values represent the cumulative risk based on the average risk per turbine in the specific wind farms intersected by the eagles. The order of eagle IDs on the x-axis is equal to the two previous figures.

Even though there are some variations in both wind farm intersection (unique and total) and cumulative collision risk, it is worth noting that there were also variations in the extents of the movement patterns. Some eagles moved north-south several times while others only completed one trip. Some eagles also stayed somewhat closer to their natal area at the island of Smøla relative to others, only moving about 100-200 km. The differences in the tracking period also varied between approximately 6 months to 3.5 years between the individuals, which naturally will have a significant effect on the differences in total cumulative collision risk.

4. Discussion

4.1 Interpretation and comparison with previous research

4.1.1 Resource selection modelling

In this thesis, the landscape of risk for white-tailed eagles was presented based on the model results of their resource selection, risk flight height and direct turbine collision risk. These results were further examined to estimate the collision risk of existing wind farms, and the cumulative risk for each tracked individual. The resource selection model suggested that sub-adult eagles are more likely to be found in uninhabited lowland regions along the coast with little vegetation, similar to findings in previous studies (Balotari-Chiebao et al., 2018; Balotari-Chiebao et al., 2021; May et al., 2013; May et al., 2021; Tikkanen et al., 2018). The eagles were also likely to appear in areas with high terrain steepness, which aligns nicely with the species flight behavior (Hanssen et al., 2020). Given their commonly used soaring flight behavior, white-tailed eagles are often attracted to orographic updrafts (Hanssen et al., 2020). These updrafts occur when wind currents are lifted vertically by steep terrain and are commonly used by soaring raptors for energy-efficient altitude gains (Bohrer et al., 2012). This could be the main reason why the eagles preferred these areas. This could also be the reason why eagles preferred coastal landscapes, as the topography along the Norwegian coast often gets steep very quickly.

When modelling these movement data, is worth noting that a large proportion of the GPS registrations in this analysis are from around the Smøla archipelago, where the transmitters were fitted to the nestlings. As a result, the eagles may be influenced by locally adapted habitat preferences within this specific population. In other words, the data do not necessarily represent the habitat preferences of white-tailed eagles in general. Nevertheless, the preferences for the different habitat categories coincide very well with previous studies elsewhere. This includes a preference for wetlands and bare rock, and an avoidance towards agriculture, urban areas, and waterbodies (Balotari-Chiebao et al., 2021; May et al., 2013; Radović & Mikuska, 2009; Tikkanen et al., 2018). Even though both marine and inland waters are important hunting grounds for white-tailed eagles (Evans et al., 2010), the avoidance of waterbodies is most likely linked to their typical hunting strategies. White-tailed eagles are known as “sit-and-wait” foragers, which minimizes the need for persistent flight activity, and greatly reduces the time spent on aerial hunting over waterbodies (Nadjafzadeh et al., 2015; Olsen et

al., 2013). In this way, the eagles spend little time flying over water, which might explain the results suggesting avoidance of these habitats.

4.1.2 Flight risk modelling

A flight risk model was also conducted, showing the predicted probabilities of an eagle flying at risk height (50 – 185 m). Here, other environmental variables came into play, showing little correlation with the results of the resource selection model. Eagles were more likely to fly at risk heights in higher altitude areas, inland waters, and forests, where they are less likely to appear. This contributes to limit the overall risk of collision in the most preferable habitats. However, a higher probability of eagles flying at risk heights over forest are expected, considering that they need to fly over the treetops. This increases the risk of reaching the collision risk zone (50 – 185 m). The only predictor standing out for both high probability of eagle presence and increased probability of flying at risk heights is slope. Bohrer et al. (2012) suggest that golden eagles use the orographic uplifts extensively for migration, and that these uplifts could be affected by the construction of wind turbines at the mountain ridges. After inspection of the turbine placements in Norwegian wind farms, many of the outermost placed turbines are located relatively close to steep slopes. This could increase the collision risk, even though the turbines are not placed directly in the slopes. Moreover, there are uncertainties related to the eagles behavioral responses in the face of wind turbines, with some studies suggesting that there are some signs of avoidance behavior (Hull & Muir, 2013; Johnston et al., 2014; Therkildsen et al., 2021), while others suggest no avoidance (Dahl et al., 2013; Grünkorn et al., 2017; Krone & Treu, 2018). Regardless, under the assumptions of no avoidance, the collision risk is likely to be higher in steep areas with turbine placements on the mountain ridges above.

4.1.3 Collision risk modelling

Given their widely used soaring flight behavior, white-tailed eagles are likely to be attracted by turbulent wind masses, regardless of origin (Spaar, 1997; Ueta & Fukuda, 2010). This claim is supported by the fact that there is an increased probability of flights occurring within the rotor-swept zone (RSZ), where air currents are drastically changed (Dahl et al., 2013). Unsurprisingly, the collision risk for white-tailed eagles is also highly associated with the number of flights withing the RSZ (May et al., 2010; May et al., 2011). Therefore, use of a collision risk model based on both

technical, biological, and environmental variables is unquestionably a crucial part of a total collision risk assessment. The model from Tucker (1996) incorporates realistic parameters which might be easily worked around through rough assumptions in other collision risk studies. The model in May et al. (2010) assumed that the eagles always approached the turbines by upwind or downwind, ignoring the possible effects of crosswind approaches. Therefore, by accounting for all possible wind speed directions, the model from Tucker (1996) is likely to provide a more realistic description of the direct collision risk. Moreover, the Tucker-model excludes assumptions of possible turbine avoidance behavior (Masden & Cook, 2016), which is likely to limit uncertainties. This becomes particularly clear when the discrepancies linked to whether eagles practice avoidance behavior at all in the face of wind turbines are considered. However, despite the realistic methodology, it is worth noting that this model also has its limitations, which is further described in chapter 4.4.

4.2 Collision risk findings

The total risk levels associated with each wind farm was strongly linked to the total number of turbines, which is expected. In other words, larger wind farms were usually associated with a higher collision risk, simply due to the magnitude of the installations. This implies that a large-scale wind farm in a low collision risk area will usually have a higher total collision risk compared to a smaller wind farm in a high risk area. As a result, the lower overall collision risk in northern wind farms is likely linked to the fact that these wind farms have a lower average number of turbines, compared to those in the south. Nevertheless, the model results suggest that many of these low total risk wind farms have been poorly sited, often located within preferable eagle habitats. As a result, these wind farms have a substantially higher collision risk per MW installed capacity, compared to the total risk. These findings match the results of May et al. (2021), who found that smaller wind farms were on average sited less effectively with a higher impact per installed capacity.

For some of the larger wind farms, minimum risk with maximum production has been achieved to a greater extent, indicated by the low risk per MW compared to the total risk. This suggest that these wind farms have been more effectively sited in less preferable and low collision risk habitats. May et al. (2021) found similar results, where larger wind farms had greater total impact of birdlife on average but were more effectively sited (indicated by a lower impact per installed capacity). As a result, the collision risk per MW installed provides a good indication of the quality of the impact

assessment and the use of preventive measures when these wind farms were sited. It also gives the decision makers an opportunity to assess the need for preventive measures in future developments in similar landscapes. For the variation in collision risk across wind farms, elevation was especially important, as the probability of eagle presence drastically decreased with increasing altitude. Ten wind farms are located above 400 meters, where eagle presence was very scarce. All of which had a relatively low collision risk per MW installed capacity, even though most of them were located on highly preferable habitat types. This clearly indicates that elevation explains a larger amount of variation in eagle presence than the habitat categories, which in turn has a substantial effect on collision risk. The eagles also had a lower probability of flying at risk heights on hilltops compared to valleys, which could contribute to the overall lower collision risk in more elevated wind farm locations.

When assessing the collision risk for each individual eagle, there was great variability in both the number of wind farm crossings (to unique wind farms and in total) and the subsequent cumulative collision risk. This variation can be influenced by several factors, including the extent of the northern movement patterns. Longer and more frequent movements would obviously have increased the number of possible wind farm intersections compared to the more limited movement patterns. First and foremost, this variation in movement patterns is most likely strongly linked to the extent of the tracking intervals between each individual. However, given the fact that eagles can travel long distances over short periods, some of the variation could also be explained by differences in individual response in the face of wind power installations. In this study, the nestling tagging was carried in and around Smøla wind farm, which is known to have a displacement effect on the local population (May et al., 2013). As a result, some variation in movement patterns may be a consequence of how different individuals respond to the displacement, if they respond at all. The movement differences could also be largely explained by how the individuals respond to ecological and demographic variables, including population density, prey availability, local weather conditions and general habitat quality.

4.3 Implications for future wind power development

4.3.1 Predictive mapping in risk assessment and optimal siting

The process of mapping the predicted collision risks across the landscape can serve as an important tool for future wind farm development. By providing a spatially explicit visualization of predicted collision risk, the identification of high risk vs. low risk areas will be optimized. In this way, the

predictive maps can allow for more effective onshore wind power site selection, limiting the collision risk. For instance, as the probability of eagle presence (and subsequent collision risk) rapidly decreases with increasing altitude, siting new wind farms at higher altitude areas might be optimal for the preservation of white-tailed eagle populations. Predictive collision risk maps can also be an important tool in streamlining the process of conducting comprehensive impact assessments linked to new wind power installations. The effectiveness and quality of environmental impact assessments can be heavily contingent on site-specific data (Ross & Evans, 2002; Tarazona, 2014). However, as these data can be difficult to obtain, researchers must sometimes settle for environmental data at a broader scale, limiting the accuracy of the assessment (Bourgeron et al., 1999; Ross & Evans, 2002; Walston et al., 2012). The predictive risk map provides localized data on collision risk, allowing for more precise assessments in relation to the impacts on white-tailed eagle populations. The map can also help to distinguish potential and undesirable project areas for wind power at an early stage in the licensing process, without the need for extensive field work in advance.

The collision risk visualizations are not only useful for selecting optimal low-risk wind power locations but can also be used for optimal placement of specific turbines within a project. The pixel size of only 50 x 50 meters allows for highly specific evaluations, encompassing the environmental variation over very short distances. In this way, the placement of turbines within a specific project can be assessed based on the local variation in collision risk. For instance, the model results suggests that turbines should be avoided close to steep slopes, as the eagles use the orographic uplift for their soaring flight (Hanssen et al., 2020). Based on the comprehensiveness, scale, and resolution of the risk map, developers and policy makers can be better suited to make informed decisions, limiting the harmful effects on white-tailed eagle populations.

4.3.2 Cumulative effects and mitigation measures

When assessing collision risk for bird species, the cumulative impacts are essential for understanding the long-term effects of wind power installations (Brabant et al., 2015; Vasilakis et al., 2017). New wind farms are expected to be functionally and economically operative for at least 25 years (NVE, 2023), suggesting that the potential cumulative collision risk effects over the next few decades might be substantial. Moreover, the Norwegian Energy Commission's study report from 2023 proposes an upscale in the current development of wind power installations to meet the European energy

requirements (Andresen et al., 2023). These ambitions require a significant foundation of knowledge related to the long-term cumulative collision risk effect for white-tailed eagles. The cumulative impacts are often neglected in environmental impact assessments, which can cause large deviations in observed vs actual degree of influence (Burris & Canter, 1993; Cooper & Sheate, 2002; Kay et al., 2010). Even though the collision risk for one wind farm might be very low, the overall impact across other existing wind farms will increase along the movement paths. Therefore, by expanding the horizon of impact to include the risk posed by several wind farms over an extended period, a more holistic risk evaluation is achieved. This can also improve the understanding of how these impacts will influence population dynamics and simplifies the process of implementing useful mitigation strategies.

The development of wind power is often characterized by a trade-off between environmental considerations and the magnitude of the production potential (Eichhorn & Drechsler, 2010). As a result, the implementation of effective mitigation strategies is a crucial part of limiting the collision risk (Garcia-Rosa & Tande, 2023). This is particularly important if the initial attempt to avoid high risk areas is inevitable. Given the substantial variation in both collision risk between wind farms and the subsequent cumulative collision risk for each individual eagle, combining different types of site-specific measures at each wind farm may be the most effective measure. This approach is also supported by previous findings (Garcia-Rosa & Tande, 2023; Marques et al., 2014). One of these measures could be to increase the visibility of the turbines by painting one of the rotor blades black, which is known to reduce collision risk (May et al., 2020). Moreover, the seasonal trend in the northern movement patterns can provide insightful information related to mitigation efforts in existing wind farms. By knowing when the eagles are expected to arrive, wind farm operations managers can implement temporal adjustments to the operation. This includes limiting or shutting down the production temporarily (Goodwin, 2018). Although this measure may prove effective in minimizing cumulative collision risk if used at several sites, it can also limit the energy production significantly (May et al., 2015). However, a new concept called SKARV could show a great potential in reducing collision risk by predicting flight trajectories with advanced detection cameras. In the event of a predicted collision, the rotor speed is only changed slightly based on the trajectory, and the production loss is minimized (Garcia-Rosa & Tande, 2023). If introduced and proven effective in several wind farms, this technology might help maintaining a healthy balance between the cumulative collision effects and sufficient production levels.

4.4 Limitations and further research

Although this study is based on an extensive dataset on eagle movement and techniques of spatial modelling, some limitation and possibilities for further research needs to be addressed. Regarding the data, the post-fledging dependency phase was removed for all individuals to limit the territorial attachment to the natal area and maximize the likelihood of northern movements. This could have a significant effect on the cumulative collision risk, as white-tailed eagles are likely to be more prone to turbine collisions in the post-fledging dependency phase (PFDP) (Balotari-Chiebao et al., 2021). However, the territorial attachment during this phase could not only influence the home range estimations but could also bias the cumulative collision risk results. Given that the natal site of most tagged individuals was close to Smøla wind farm, the probability of frequent flights through the wind farm during this phase is high. Therefore, by including these data, the cumulative risk assessment would no longer be limited to moving sub-adult individuals, which was the objective. Another possible limitation is related to the resource selection, as a large part of the eagle relocations were found around the Smøla archipelago. This could have biased the predictive resource selection model towards the landscapes of this region, which was then extrapolated to the entire study area. However, this does not necessarily mean that the resource selection would be significantly different elsewhere along the study area. The data represent a wide range of habitats and environmental variables typically found in Norwegian landscapes. As a result, the probability of a biased resource selection model and subsequent predicted collision risk is minimal.

In the collision risk model from Tucker (1996), the risk is only assessed on individual level, and does not measure an actual number of expected collisions on a population level (Masden & Cook, 2016; Tucker, 1996). However, in this thesis, the final collision risk estimates are linked to population size, as the probability of presence is used as a basis for risk estimation. This made it possible to calculate the proportion of the total population that is expected to collide in each wind farm, as explained in chapter 2.8. Still, the link between the predicted probability of presence and population density also facilitates the possibility of estimating the actual number of collisions, if the total population size across the study areas is known (Bourgeron et al., 1999). This stage was excluded in this thesis, as no effective way of upscaling from predicted collision risk to number of individuals were found. Nevertheless, the approaches used in this thesis provides a tangible result and should be considered in similar studies when total population density data are available. The model from Tucker (1996) is also influenced by some general assumptions that could affect the collision risk results. The eagles

are assumed to be gliding, and not flapping at the time of collision (Masden & Cook, 2016). The potential turbine collisions are also only expected to occur with the rotating tower blades, and not the towers themselves (Masden & Cook, 2016). However, it is worth noting that the effects of these minor assumptions are likely to be very low.

The modelling and predictive collision risk assessments in this thesis creates an insightful and important foundation for further analysis that highlights the harmful effects of wind power. The accuracy of the predicted collision risks could be enhanced by incorporating additional environmental variables. For example, local weather conditions are known to increase the risk of birds colliding with turbines due to the impact on terrain visibility (Johnson et al., 2002; Marques et al., 2014). The weather data could be included to highlight areas that have a higher probability of reduced visibility, which would then be accounted for in the total collision risk predictions. Further research could also include the changes in cumulative collision risk as the development of new wind farms continues. This would be particularly interesting if more effective mitigation strategies were implemented in both new and existing wind farms in the future. Nevertheless, there is an indefinite number of both fixed and dynamic factors influencing collision risk in wind power environments. As a result, the negative effects on white-tailed eagles and other bird populations still require additional research when the development of wind power will increase.

5. Conclusion

In this study, the total collision risk for white-tailed eagles in relation to onshore wind power were modelled and predicted across the landscape. The risk levels of existing onshore wind power installations were also analyzed, in addition to the cumulative collision risk for each individual eagle during the tracking period. The study illuminates the complexity associated with predictive collision risk, and why these findings can be essential in reducing the harmful effects on white-tailed eagle populations. Through the process of predictive modelling, pivotal environmental variables increasing the probability of eagle presence and flying at risk heights were identified. The implementation of a mathematical collision risk model also increased the level of detail in the total predictive collision risk. By knowing where the eagles are prone to increased collision risk at site-specific levels, the impact assessments for future wind farm installations may improve. The detailed nature and high resolution of the predictive maps also allowed for specific risk estimations for existing onshore wind

farms. The differences in collision risk between different sites was considerable, with certain wind farms being sited far less effective than others. These findings can increase the incentives to implement effective mitigation strategies in both existing and future wind farm developments. Additionally, the cumulative collision risk assessment revealed that a wide range moving sub-adult eagle is almost guaranteed to move through several wind farms during an extended tracking period. The risk of collision increases with each intersection, amplifying the need for site-specific mitigation measures in several wind farms. As the development is expected to increase, the importance of understanding the complex relationship between wind power and avian wildlife is rapidly growing. Hence, the use of landscape-level predictive mapping and cumulative risk assessment can function as important tools in maintaining sustainability in large-scale strategic planning. These methods represent a step in the right direction for improved nature conservation efforts and can pave the way for further impact research.

6. References

Abbasi, T., Premalatha, M., Abbasi, T. & Abbasi, S. A. (2013). Wind energy: Increasing deployment, rising environmental concerns. *Renewable and Sustainable Energy Reviews*, 31: 270-288. doi: 10.1016/j.rser.2013.11.019.

Andresen, Ø., Fredriksen, B. F., Gotaas, S., Hauglie, A., Heia, G., Lundberg, S. A., Ringkjøb, H.-E., Roland, K., Rollefsen, G., Seim, H., et al. (2023). *Mer av alt - raskere: Energikommisjonens rapport*: Olje- og Energidepartementet.

Balotari-Chiebao, F., Brommer, J. E., Saurola, P., Ijäs, A. & Laaksonen, T. (2018). Assessing space use by pre-breeding white-tailed eagles in the context of wind-energy development in Finland. *Landscape and Urban Planning* 177: 251–258. doi: 10.1016/j.landurbplan.2018.05.012.

Balotari-Chiebao, F., Brommer, J. E., Tikkanen, H. & Laaksonen, T. (2021). Habitat use by post-fledging white-tailed eagles shows avoidance of human infrastructure and agricultural areas. *European Journal of Wildlife Research*, 67. doi: 10.1007/s10344-021-01482-6.

Barbet-Massin, M., Jiguet, F., Albert, C. H. & Thuiller, W. (2012). Selecting pseudo-absences for species distribution models: how, where and how many? *Methods in Ecology and Evolution*, 3 (2): 327-338. doi: 10.1111/j.2041-210X.2011.00172.x.

Barth, E. K. & Gjershaug, J. O. (2023). *Havørn*: Store Norske Leksikon. Available at: https://snl.no/hav%C3%B8rn (accessed: 07.05.2024).

Bartoń, K. (2023). *MuMIn: Multi-Model Inference. R package version 1.47.5*. Available at: https://CRAN.R-project.org/package=MuMIn (accessed: 13.05.2024).

Bates, D., Maechler, M., Bolker, B. & Walker, S. (2015). Fitting Linear Mixed-Effects Models Using lme4. *Journal of Statistical Software*, 67 (1): 1-48. doi: 10.18637/jss.v067.i01.

Beston, J. A., Diffendorfer, J. E., Loss, S. R. & Johnson, D. H. (2016). Prioritizing Avian Species for Their Risk of Population-Level Consequences from Wind Energy Development. *Plos One*, 11 (3). doi: 10.1371/journal.pone.0150813.

Bohrer, G., Brandes, D., Mandel, J. T., Bildstein, K. L., Miller, T. A., Lanzone, M., Katzner, T., Maisonneuve, C. & Tremblay, J. A. (2012). Estimating updraft velocity components over large spatial scales: contrasting migration strategies of golden eagles and turkey vultures. *Ecology letters*, 15 (2): 96-103. doi: 10.1111/j.1461-0248.2011.01713.x.

Bolker, B. M., Brooks, M. E., Clark, C. J., Geange, S. W., Poulsen, J. R., Stevens, M. H. H. & White, J.-S. S. (2008). Generalized linear mixed models: a practical guide for ecology and evolution. *Trends in Ecology & Evolution*, 24 (3): 127-135. doi: 10.1016/j.tree.2008.10.008.

Bourgeron, P. S., Humphries, H. C., Barber, J. A., Turner, S. J., Jensen, M. E. & Goodman, I. A. (1999). Impact of Broad- and Fine-Scale Patterns on Regional Landscape Characterization Using AVHRR-Derived Land Cover Data. *Ecosystem Health*, 5 (4): 234-258. doi: 10.1046/j.1526-0992.1999.09943.x.

Brabant, R., Vanermen, N., Stienen, E. W. M. & Degraer, S. (2015). Towards a cumulative collision risk assessment of local and migrating birds in North Sea offshore wind farms. *Hydrobiologia*, 756 (1): 63-74. doi: 10.1007/s10750-015-2224-2.

Buchin, K., Sijben, S., Loon, E. E. v., Sapir, N., Mercier, S., Arseneau, T. J. M. & Willems, E. P. (2015). Deriving movement properties and the effect of the environment from the Brownian

bridge movement model in monkeys and birds. *Movement Ecology*, 3 (1): 18-18. doi: 10.1186/s40462-015-0043-8.

Burnham, K. P. & Anderson, D. R. (2004). Multimodel Inference: Understanding AIC and BIC in Model Selection. *Sociological Methods & Research*, 33 (2): 261-304. doi: 10.1177/0049124104268644.

Burris, R. K. & Canter, L. W. (1993). Cumulative impacts are not properly addressed in environmental assessments. *Environmental Impact Assessment Review*, 17 (1): 5-18. doi: 10.1016/S0195-9255(96)00082-0.

Calenge, C. & Fortmann-Roe, S. (2023). *adehabitatHR: Home Range Estimation. R package version 0.4.21*. Available at: https://CRAN.R-project.org/package=adehabitatHR.

Cooper, L. M. & Sheate, W. R. (2002). Cumulative effects assessment: A review of UK environmental impact statements. *Environmental Impact Assessment Review*, 22 (4): 415-439. doi: 10.1016/S0195-9255(02)00010-0.

Dahl, E. L., May, R., Hoel, P. L., Bevanger, K., Pedersen, H. C., Røskaft, E. & Stokke, B. G. (2013). White-Tailed Eagles (Haliaeetus albicilla) at the Smøla Wind-Power Plant, Central Norway, Lack Behavioral Flight Responses to Wind Turbines. *Wildlife Society Bulletin* 37 (1): 66-74. doi: 10.1002/wsb.258.

Drewitt, A. L. & Langston, R. H. W. (2006). Assessing the impacts of wind farms on birds. *Special Issue: Wind, Fire and Water: Renewable Energy and Birds*, 148 (s1): 29-42. doi: 10.1111/j.1474-919X.2006.00516.x.

Eichhorn, M. & Drechsler, M. (2010). Spatial Trade-Offs between Wind Power Production and Bird Collision Avoidance in Agricultural Landscapes. *Ecology and Society*, 15 (2).

Evans, R. J., Pearce-Higgins, J., Whitfield, D. P., Grant, J. R., MacLennan, A. & Reid, R. (2010). Comparative nest habitat characteristics of sympatric White-tailed Haliaeetus albicilla and Golden Eagles Aquila chrysaetos in western Scotland. *Bird Study*, 57 (4): 473-482. doi: 10.1080/00063657.2010.489317.

Fischer, J. W., Walter, W. D. & Avery, M. l. (2013). Brownian Bridge Movement Models to characterize birds' home ranges. *The Condor*, 115 (2): 298-305. doi: 10.1525/cond.2013.110168.

Forthofer, R. N., Lee, E. S. & Hernandez, M. (2007). 13 - Linear Regression. In *Biostatistics (Second Edition)*, pp. 349-386.

Fox, J. & Weisberg, S. (2019). An R Companion to Applied Regression, Third Edition.

Garcia-Rosa, P. B. & Tande, J. O. G. (2023). Mitigation measures for preventing collision of birds with wind turbines. *Journal of Physics: Conference Series*. doi: 10.1088/1742-6596/2626/1/012072.

Garvin, J. C., Jennelle, C. S., Drake, D. & Grodsky, S. M. (2010). Response of raptors to a windfarm. *Journal of Applied Ecology*, 48 (1): 199-209. doi: 10.1111/j.1365-2664.2010.01912.x.

Goodwin, W. (2018). Alternative methods to mitigate wind turbine collisions for vultures and other soaring birds. *Vulture News*, 73. doi: 10.4314/vulnew.v73i1.3.

Grünkorn, T., Gippert, M., Treu, G. & Nehls, G. (2017). *Behavioural Observations of White-Tailed Sea Eagles in the Vicinity of Wind Turbines*. Birds of Prey and Wind Farms.

Halgunset, G. S. (2023). *Project description for master thesis - Term paper in MINA310 - Methods in Natural Sciences*.

Hanssen, F., May, R. & Nygård, T. (2020). High-Resolution Modeling of Uplift Landscapes can Inform - Micrositing of Wind Turbines for Soaring Raptors. *Environmental Management*, 66: 319–332. doi: 10.1007/s00267-020-01318-0.

Hardey, J., Crick, H., Wernham, C., Riley, H., Etheridge, B. & Thompson, D. (2006). *Raptors: a field guide to survey and monitoring*. Edinburgh: The Stationary Office Limited.

Hebblewhite, M. & Merrill, E. (2008). Modelling wildlife–human relationships for social species with mixed-effects resource selection models. *Journal of Applied Ecology*, 45 (3): 834-844. doi: 10.1111/j.1365-2664.2008.01466.x.

Hendrickx, J. & Utrecht, D. N. (2018). *Collinearity in Mixed Models*. The Netherlands.

Heuck, C., Herrmann, C., Levers, C., Leitão, P. J., Krone, O., Brandl, R. & Albrecht, J. (2019). Wind turbines in high quality habitat cause disproportionate increases in collision mortality of the white-tailed eagle. *Biological Conservation*, 236: 44-51. doi: 10.1016/j.biocon.2019.05.018.

Hijmans, R. J. (2023). *raster: Geographic Data Analysis and Modeling. R package version 3.6-26*. Available at: https://CRAN.R-project.org/package=raster (accessed: 25.04.2024).

Holmstroma, L. A., Hamera, T. E., Colclaziera, E. M., Denisa, N., P.Verschuylb, J. & Ruché, D. (2011). Assessing Avian-Wind Turbine Collision Risk: An Approach Angle Dependent Model. *Wind Engineering*, 5 (3): 289-312. doi: 10.1260/0309-524X.35.3.289.

Hull, C. L. & Muir, S. C. (2013). Behavior and turbine avoidance rates of eagles at two wind farms in Tasmania, Australia. *Wildlife Society Bulletin*, 37 (1): 49-58. doi: 10.1002/wsb.254.

Johnson, G. D., Erickson, W. P., Strickland, M. D., Shepherd, M. F., Shepherd, D. A. & Sarappo, S. A. (2002). Collision Mortality of Local and Migrant Birds at a Large-Scale Wind-Power Development on Buffalo Ridge, Minnesota. *Wildlife Society Bulletin*, 30 (3): 879-887.

Johnston, N., Bradley, J. E. & Otter, K. (2014). Increased Flight Altitudes among Migrating Golden Eagles Suggest Turbine Avoidance at a Rocky Mountain Wind Installation. *Plos One*, 9 (3): e93030-e93030. doi: 10.1371/journal.pone.0093030.

Kartverket. (2023). *Høgdedata og djupnedata*. Available at: https://www.kartverket.no/api-og-data/terrengdata (accessed: 25.09.2023).

Kay, D., Geisler, C. & Stedman, R. C. (2010). What is Cumulative Impact Assessment and Why Does it Matter? *Research & Policy Brief Series* (37).

Kikuchi, R. (2008). Adverse impacts of wind power generation on collision behaviour of birds and anti-predator behaviour of squirrels. *Journal for Nature Conservation*, 16: 44-55. doi: 10.1016/j.jnc.2007.11.001.

Kroglund, R. T. (2022). *Ørner*. Available at: https://snl.no/%C3%B8rner (accessed: 11.04.2023).

Krone, O. & Treu, G. (2018). Movement patterns of white-tailed sea eagles near wind turbines. *The Journal of Wildlife Management*, 82 (2): 1367-1375. doi: 10.1002/jwmg.21488.

Lüdecke, D. (2018). ggeffects: Tidy Data Frames of Marginal Effects from Regression Models. *Journal of Open Source Software*, 3 (26): 772. doi: 10.21105/joss.00772.

Madders, M. & Whitfield, D. P. (2006). Upland raptors and the assessment of wind farm impacts. *Ibis*, 148 (1): 43-56. doi: 10.1111/j.1474-919X.2006.00506.x.

Marques, A. T., Batalha, H., Rodrigues, S., Costa, H., João, M., Pereira, R., Fonseca, C., Mascarenhas, M. & Bernardino, J. (2014). Understanding bird collisions at wind farms: An updated review on the causes and possible mitigation strategies. *Biological Conservation*, 179: 40-52. doi: 10.1016/j.biocon.2014.08.017.

Martínez, J. E., Calvo, J. F. & Zuberogoitia, I. (2010). Potential impact of wind farms on territories of large eagles in southeastern Spain. *Biodiversity and Conservation*, 19 (13): 3757-3767. doi: 10.1007/s10531-010-9925-7.

Masden, E. A. & Cook, A. S. C. P. (2016). Avian collision risk models for wind energy impact assessments. *Environmental Impact Assessment Review*, 56: 43-49. doi: 10.1016/j.eiar.2015.09.001.

May, R., Hoel, P. L., Langston, R., Dahl, E. L., Bevanger, K., Reitan, O., Nygård, T., Pedersen, H. C., Røskaft, E. & Stokke, B. G. (2010). *Collision risk in white-tailed eagles - Modelling collision risk using vantage point observations in Smøla wind-power plant* NINA Report.

May, R., Nygård, T., Dahl, E. L., Reitan, O. & Bevanger, K. (2011). *Collision risk in white-tailed eagles - Modelling kernel-based collision risk using satellite telemetry data in Smøla wind-power plant*. NINA Report 692.

May, R., Nygård, T., Dahl, E. l. & Bevanger, K. (2013). Habitat Utilization in White-Tailed Eagles (Haliaeetus albicilla) and the Displacement Impact of the Smøla Wind-power Plant. *Wildlife Society Bulletin*, 37 (1): 75-83. doi: 10.1002/wsb.264.

May, R., Reitan, O., Bevanger, K., Lorentsen, S.-H. & Nygård, T. (2015). Mitigating wind-turbine induced avian mortality: Sensory, aerodynamic and cognitive constraints and options. *Renewable and Sustainable Energy Reviews*, 42: 170-181. doi: 10.1016/j.rser.2014.10.002.

May, R., Nygård, T., Falkdalen, U., Åström, J., Hamre, Ø. & Stokke, B. G. (2020). Paint it black: Efficacy of increased wind turbine rotor blade visibility to reduce avian fatalities. *Ecology and Evolution*, 10 (16): 8927-8935. doi: 10.1002/ece3.6592.

May, R., Jackson, C. R., Middel, H., Stokke, B. G. & Verones, F. (2021). Life-cycle impacts of wind energy development on bird diversity in Norway. *Environmental Impact Assessment Review*, 90. doi: 10.1016/j.eiar.2021.106635.

Merkle, J. A., Krausman, P. R., Decesare, N. J. & Jonkel, J. J. (2011). Predicting spatial distribution of human–black bear interactions in urban areas. *The Journal of Wildlife Management*, 75 (5): 1121-1127. doi: 10.1002/jwmg.153.

Morris, L. R., Proffitt, K. M. & Blackburn, J. K. (2016). Mapping resource selection functions in wildlife studies: Concerns and recommendations. *Applied Geography*, 76: 173-183. doi: 10.1016/j.apgeog.2016.09.025.

Nadjafzadeh, M., Hofer, H. & Krone, O. (2015). Sit-and-wait for large prey: foraging strategy and prey choice of White-tailed Eagles. *Journal of Ornithology*, 157 (1): 165-178. doi: 10.1007/s10336-015-1264-8.

NIBIO. (2024). *Nedlasting av kartdata - Last ned kartfiler for bruk i egne kartprogram*. Available at: https://www.nibio.no/tjenester/nedlasting-av-kartdata (accessed: 07.01.2024).

NVE. (2023). *Forutsetninger for estimering av kostnader for kraftproduksjon*

NVE. (2024a). *Kunnskapsgrunnlag om virkninger av vindkraft på land - Støy*. Available at: https://www.nve.no/energi/energisystem/vindkraft/kunnskapsgrunnlag-om-virkninger-av-vindkraft-paa-land/stoey/ (accessed: 14.03.2024).

NVE. (2024b). *Nedlasting av fagdata fra NVE*: Norges vassdrags- og energidirektorat. Available at: https://nedlasting.nve.no/gis/ (accessed: 25.03.2024).

Nygård, T., Bevanger, K., Dahl, E. L., Flagstad, Ø., Follestad, A., Hoel, P. L., May, R. & Reitan, O. (2010). A study of White-tailed Eagle Haliaeetus albicilla movements and mortality at a wind farm in Norway.

Olsen, J., Debus, S. J. S., Rose, A. B. & Judge, D. (2013). Nest-sites and foraging of the White-bellied Sea-Eagle 'Haliaeetus leucogaster' on the subtropical eastern coast of Australia. *Australian Field Ornithology*, 29: 149–159.

QGIS.org. (2024). *QGIS Geographic Information System*: QGIS Association. Available at: http://www.qgis.org.

Radović, A. & Mikuska, T. (2009). Population size, distribution and habitat selection of the white-tailed eagle Haliaeetus albicilla in the alluvial wetlands of Croatia. *Biologia*, 65 (1): 156-164. doi: 10.2478/s11756-009-0011-0.

Ross, S. & Evans, D. (2002). Excluding site-specific data from the lca inventory: how this affects life cycle impact assessment. *The International Journal of Life Cycle Assessment*, 7 (3): 141-150. doi: 10.1007/BF02994048.

RStudio. (2015). *RStudio: Integrated Development for R. RStudio*. Bonton, MA: PBC. Available at: http://www.rstudio.com/.

Spaar, R. (1997). Flight strategies of migrating raptors; a comparative study of interspecific variation in flight characteristics *International journal of aviation science*, 139 (3): 523-535. doi: 10.1111/j.1474-919X.1997.tb04669.x.

Stokmo, J. A. (2021). *Kongeørn fløy 180 kilometer på et døgn*. Available at: https://forskning.no/dyrevelferd-fugler-miljoovervakning/kongeorn-floy-180-kilometer-pa-et-dogn/1827764 (accessed: 11.04.2023).

Tarazona, J. V. (2014). *Site-Specific Environmental Risk Assessment*. Encyclopedia of Toxicology (Third Edition).

Therkildsen, O. R., Balsby, T. J. S., Kjeldsen, J. P., Nielsen, R. D., Bladt, J. & Fox, A. D. (2021). Changes in flight paths of large-bodied birds after construction of large terrestrial wind turbines. *Journal of Environmental Management*, 290. doi: 10.1016/j.jenvman.2021.112647.

Tikkanen, H., Balotari-Chiebao, F., Laaksonen, T., Pakanen, V.-M. & Rytkönen, S. (2018). Habitat use of flying subadult White-tailed Eagles (Haliaeetus albicilla): implications for land use and wind power plant planning. *Ornis Fennica*, 95: 137-150. doi: 10.51812/of.133937.

Tucker, V. A. (1996). A Mathematical Model of Bird Collisions With Wind Turbine Rotors. *Journal of Solar Energy Enginering*, 118 (4): 253-262. doi: 10.1115/1.2871788.

Ueta, M. & Fukuda, Y. (2010). Effect of meteorological factors on frequency of flight for White-tailed and Steller's Sea Eagles along sea coast. *Bird Reseach*, 6: 21-26. doi: 10.11211/birdresearch.6.S21.

Vargas, S. A., Esteves, G. R. T., Maçaira, P. M., Bastos, B. Q., Oliveira, F. L. C. & Souza, R. C. (2019). Wind power generation: A review and a research agenda. *Journal of Cleaner Production*, 218: 850-870. doi: 10.1016/j.jclepro.2019.02.015.

Vasilakis, D. P., Whitfield, D. P. & Kati, V. (2017). A balanced solution to the cumulative threat of industrialized wind farm development on cinereous vultures (*Aegypius monachus*) in south-eastern Europe. *Plos One*, 12 (2). doi: 10.1371/journal.pone.0172685.

Walker, D., Mcgrady, M., Mccluskie, A., Madders, M. & Mcleod, D. R. A. (2005). Resident Golden Eagle ranging behaviour before and after construction of a windfarm in Argyll. *Scottish Birds*, 25: 24-40.

Walston, L. J., Lagory, K. E., Vinikour, W., Lonkhuyzen, R. L. V. & Cantwell, B. (2012). Improving landscape-level environmental impact evaluations. *Esri*.

Young, J., Watt, A., Nowicki, P., Alard, D., Clitherow, J., Henle, K., Johnson, R., Laczko, E., McCracken, D., Matouch, S., et al. (2005). Towards sustainable land use: identifying and managing the conflicts between human activities and biodiversity conservation in Europe. *Biodiversity & Conservation*, 14: 1641–1661. doi: 10.1007/s10531-004-0536-z.

Appendices

Appendix A: Aggregated land cover types

Aggregated land cover types from Corine Land Cover 2018.

CLC-code	Aggregated cover type
1.1.1 Continuous urban fabric	Urban
1.1.2 Discontinuous urban fabric	
1.2.1 Industrial or commercial units	
1.2.2 Road and rail network and associated land	
1.2.3 Port areas	
1.2.4 Airports	
1.3.1 Mineral extraction sites	
1.3.2 Dump sites	
1.3.3 Contruction sites	
1.4.1 Green urban areas	
1.4.2 Sport and leisure facilities	
2.1.1 Non-irrigated arable land	Agricultural
2.1.2 Permanently irrigated land	
2.1.3 Rice fields	
2.2.1 Vineyards	
2.2.2 Fruit trees and berry plantations	
2.2.3 Olive groves	
2.3.1 Pastures	
2.4.1 Annual crops assosiated with permanent crops	
2.4.2 Complex cultivation	
2.4.3 Land principally occupied by agriculture, with significant areas of natural vegetation	
2.4.4 Agro-forestry areas	
3.1.1 Broad-leaved forest	Forest
3.1.2 Coniferous forest	
3.1.3 Mixed forest	
3.2.1 Natural grassland	Shrubland
3.2.2 Moors and heath land	
3.2.3 Sclerophyllous vegetation	
3.2.4 Transitional woodland/shrub	
3.3.1 Beaches, dunes and sand plains	Bare rock / Scarcely vegetated
3.3.2 Bare rock	
3.3.3 Sparsely vegetated areas	
3.3.4 Burnt areas	
3.3.5 Glacier and prepetual snow	
4.1.1 Inland marhes	Wetland
4.1.2 Peat bogs	
4.2.1 Salt marshes	
4.2.2 Salines	
4.2.3 Intertidal flats	
5.1.1 Water cources	Inland waters
5.1.2 Water bodies	
5.2.1 Coastal lagoons	Ocean waters
5.2.2 Estauries	
5.2.3 Sea and ocean	

Appendix B: Home range polygons

Home ranges for each individual white-tailed eagle included in the analysis. The color-range represents the proportion of relocations found within these areas.

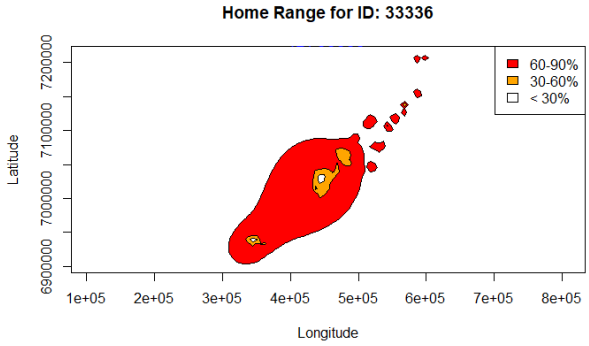

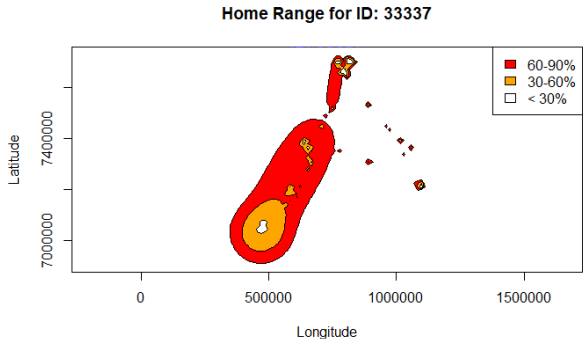

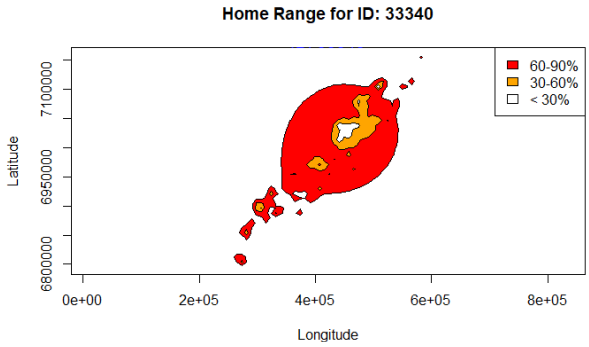

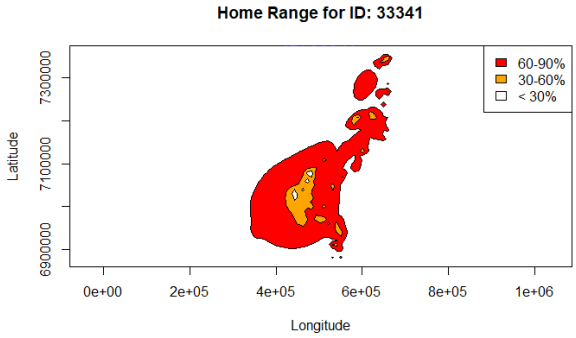

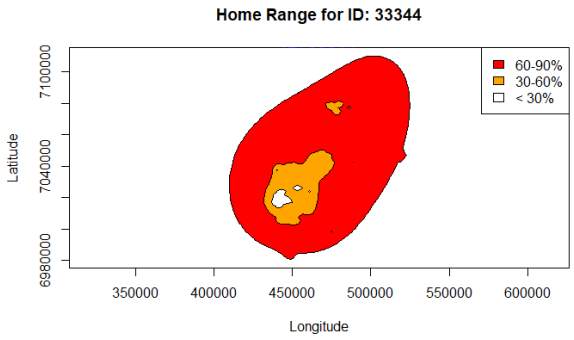

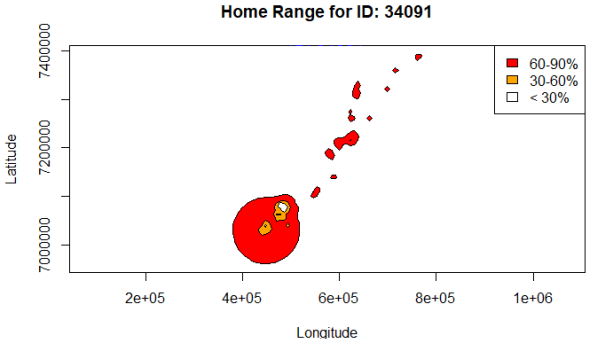

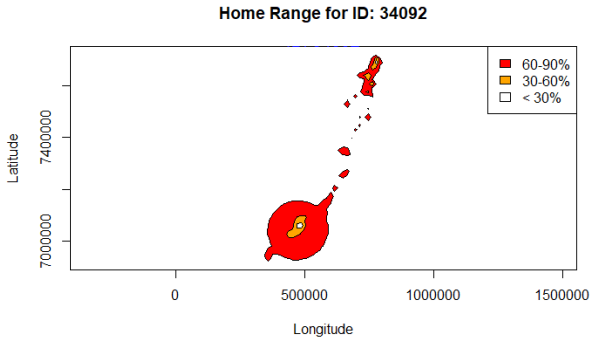

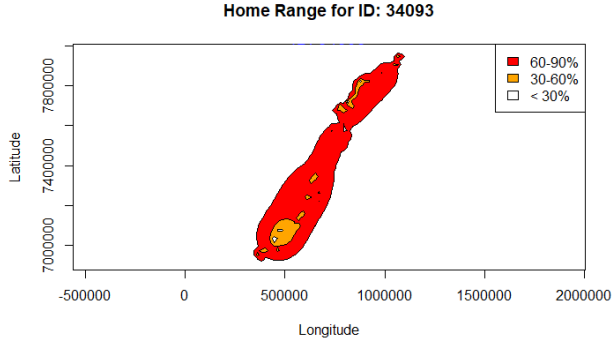

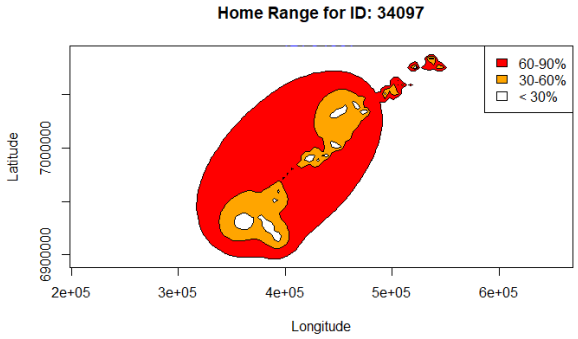
Home Range for ID: 34097
60-90%
30-60%
< 30%
Latitude
6900000
7000000
2e+05
3e+05
4e+05
5e+05
6e+05
Longitude

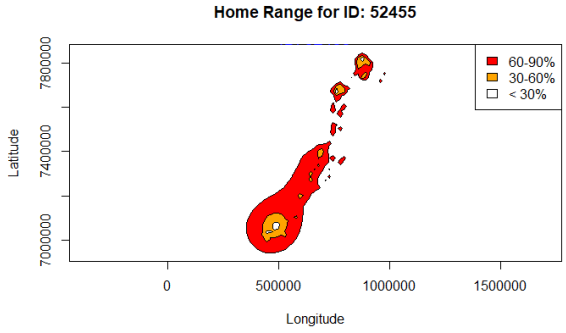
Home Range for ID: 52455
60-90%
30-60%
< 30%
Latitude
7000000
7400000
7800000
0
500000
1000000
1500000
Longitude

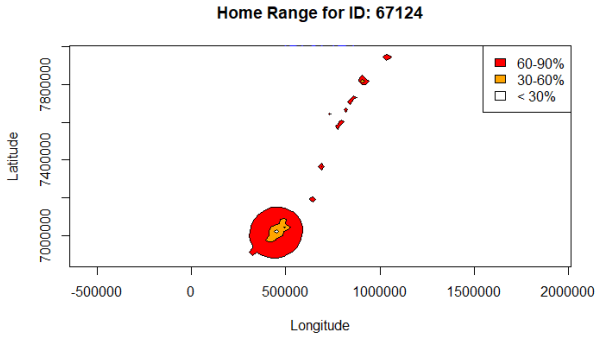
Home Range for ID: 67124
60-90%
30-60%
< 30%
Latitude
7000000
7400000
7800000
-500000
0
500000
1000000
1500000
2000000
Longitude

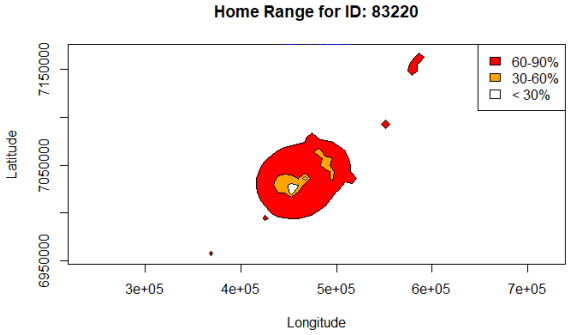
Home Range for ID: 83220
60-90%
30-60%
< 30%
Latitude
6950000
7050000
7150000
3e+05
4e+05
5e+05
6e+05
7e+05
Longitude

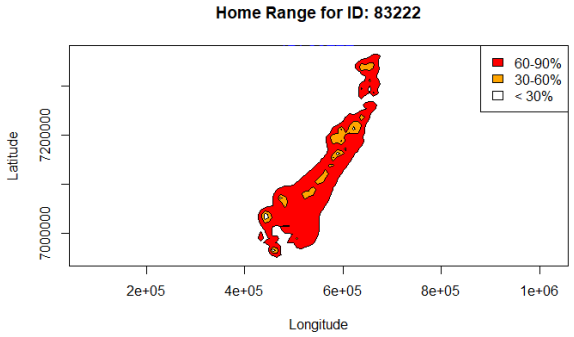
Home Range for ID: 83222
60-90%
30-60%
< 30%
Latitude
7000000
7200000
2e+05
4e+05
6e+05
8e+05
1e+06
Longitude

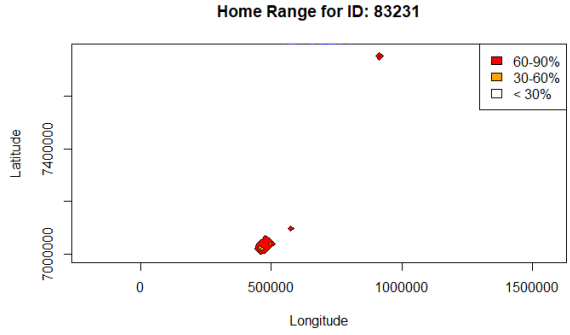
Home Range for ID: 83231
60-90%
30-60%
< 30%
Latitude
7000000
7400000
0
500000
1000000
1500000
Longitude

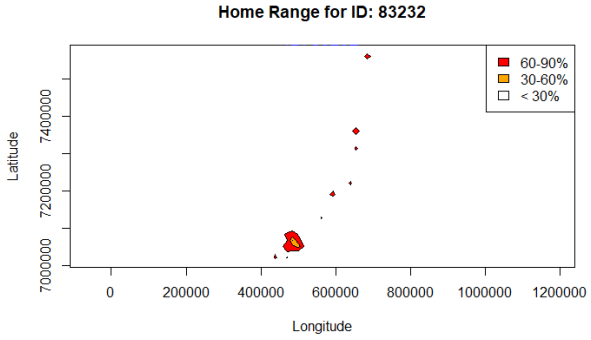
Home Range for ID: 83232
60-90%
30-60%
< 30%
Latitude
7000000
7200000
7400000
0
200000
400000
600000
800000
1000000
1200000
Longitude

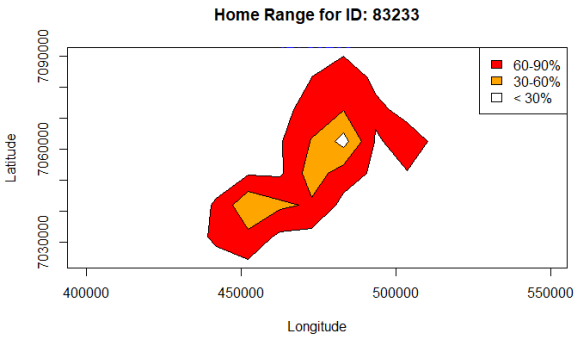
Home Range for ID: 83233
60-90%
30-60%
< 30%
Latitude
7030000
7060000
7090000
400000
450000
500000
550000
Longitude

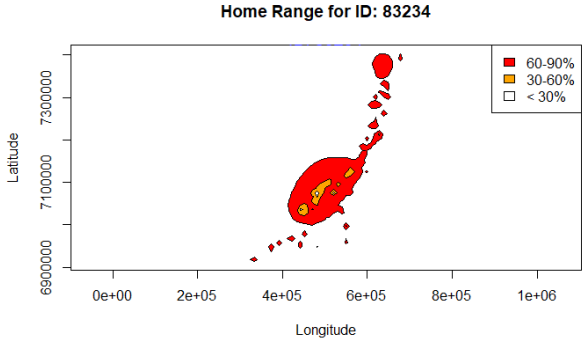
Home Range for ID: 83234
60-90%
30-60%
< 30%
Latitude
6900000
7100000
7300000
0e+00
2e+05
4e+05
6e+05
8e+05
1e+06
Longitude

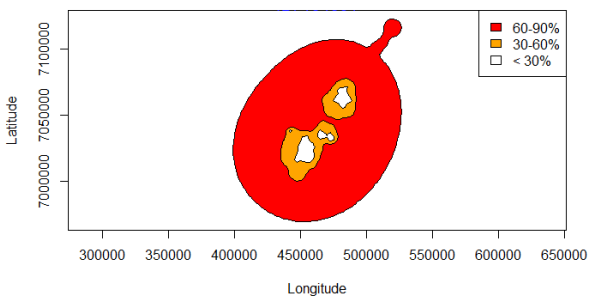
Home Range for ID: 134091
60-90%
30-60%
< 30%
Latitude
7000000
7050000
7100000
300000
350000
400000
450000
500000
550000
600000
650000
Longitude

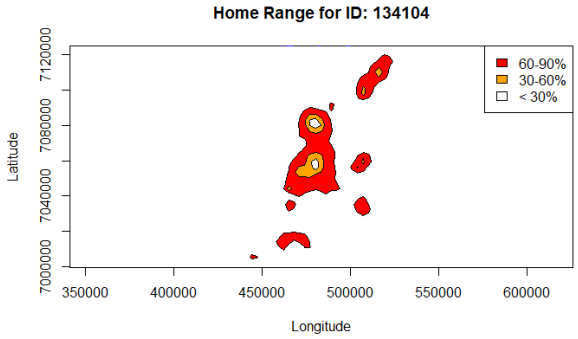
Home Range for ID: 134104
60-90%
30-60%
< 30%
Latitude
Longitude
7000000
7040000
7080000
7120000
350000
400000
450000
500000
550000
600000

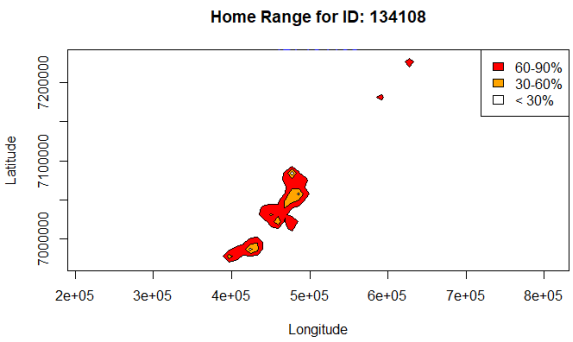
Home Range for ID: 134108
60-90%
30-60%
< 30%
Latitude
Longitude
7000000
7100000
7200000
2e+05
3e+05
4e+05
5e+05
6e+05
7e+05
8e+05

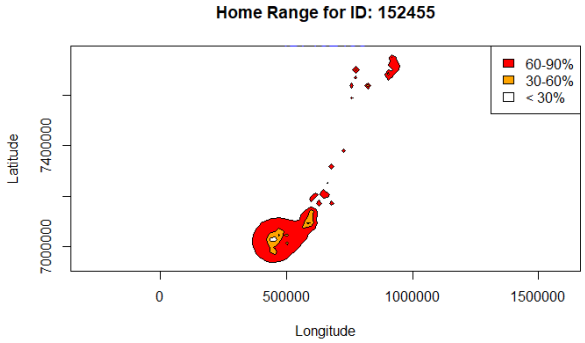
Home Range for ID: 152455
60-90%
30-60%
< 30%
Latitude
Longitude
7000000
7400000
0
500000
1000000
1500000

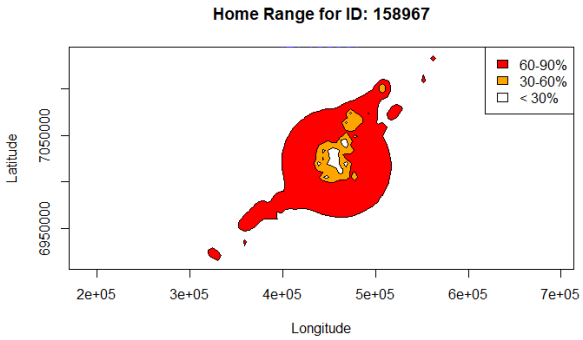
Home Range for ID: 158967
60-90%
30-60%
< 30%
Latitude
Longitude
6950000
7050000
2e+05
3e+05
4e+05
5e+05
6e+05
7e+05

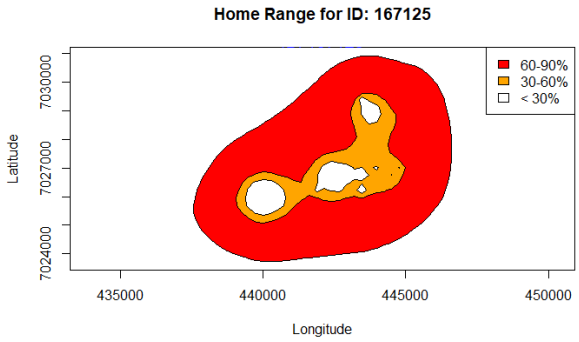
Home Range for ID: 167125
60-90%
30-60%
< 30%
Latitude
Longitude
7024000
7027000
7030000
435000
440000
445000
450000

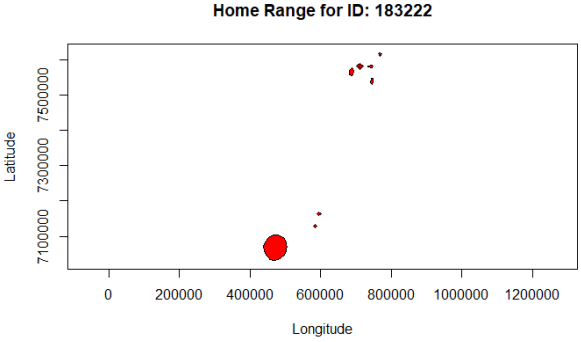
Home Range for ID: 183222
Latitude
Longitude
7100000
7300000
7500000
0
200000
400000
600000
800000
1000000
1200000

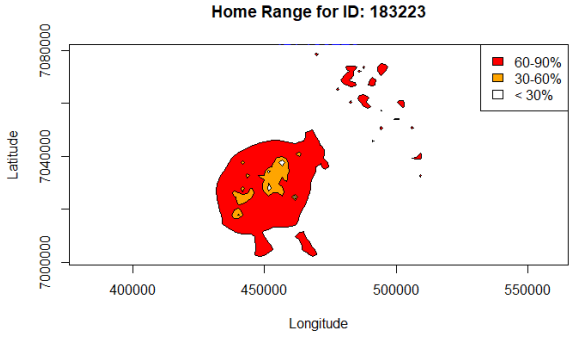
Home Range for ID: 183223
60-90%
30-60%
< 30%
Latitude
Longitude
7000000
7040000
7080000
400000
450000
500000
550000

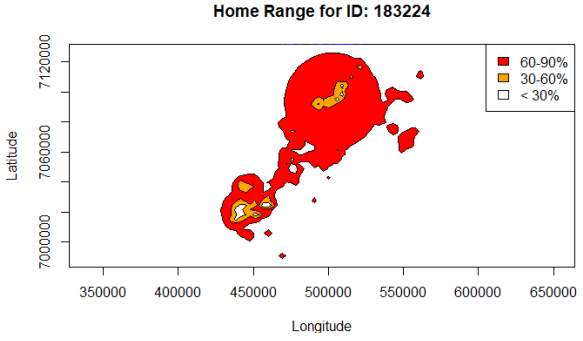
Home Range for ID: 183224
60-90%
30-60%
< 30%
Latitude
Longitude
7000000
7060000
7120000
350000
400000
450000
500000
550000
600000
650000

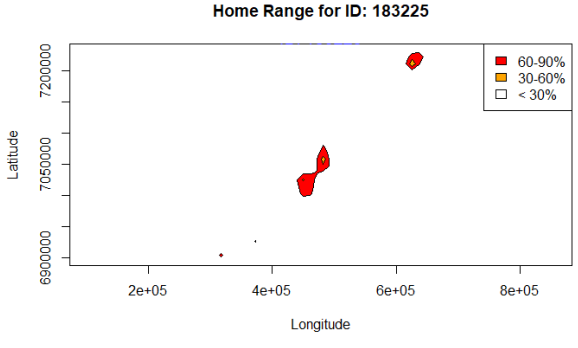
Home Range for ID: 183225
60-90%
30-60%
< 30%
Latitude
Longitude
6900000
7050000
7200000
2e+05
4e+05
6e+05
8e+05

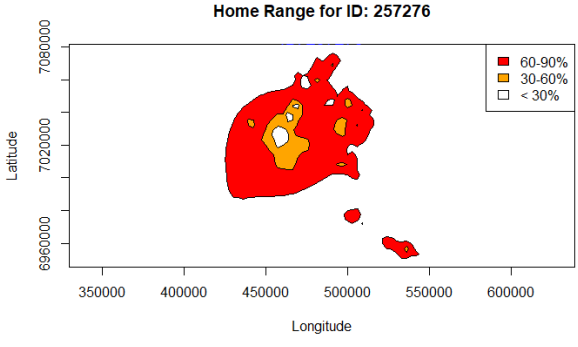
Home Range for ID: 257276
60-90%
30-60%
< 30%
Latitude
Longitude
6960000
7020000
7080000
350000
400000
450000
500000
550000
600000

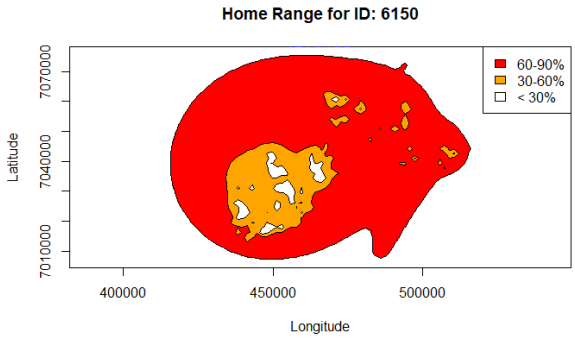
Home Range for ID: 6150
60-90%
30-60%
< 30%
Latitude
7070000
7040000
7010000
400000
450000
500000
Longitude

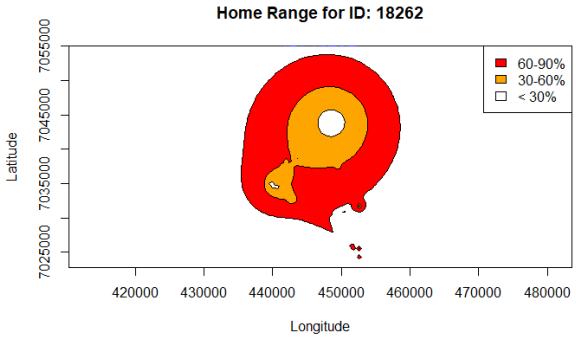
Home Range for ID: 18262
60-90%
30-60%
< 30%
Latitude
7055000
7045000
7035000
7025000
420000
430000
440000
450000
460000
470000
480000
Longitude

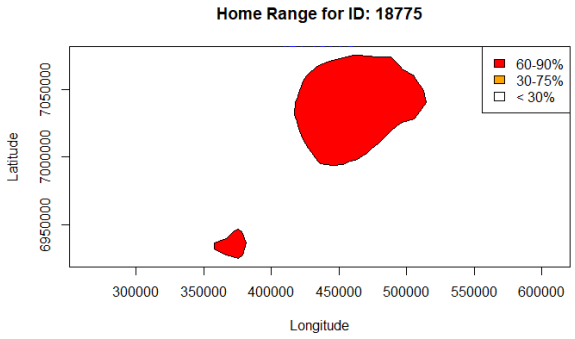
Home Range for ID: 18775
60-90%
30-75%
< 30%
Latitude
7050000
7000000
6950000
300000
350000
400000
450000
500000
550000
600000
Longitude

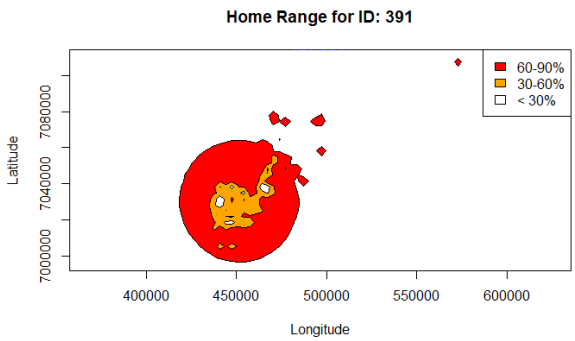
Home Range for ID: 391
60-90%
30-60%
< 30%
Latitude
7080000
7040000
7000000
400000
450000
500000
550000
600000
Longitude

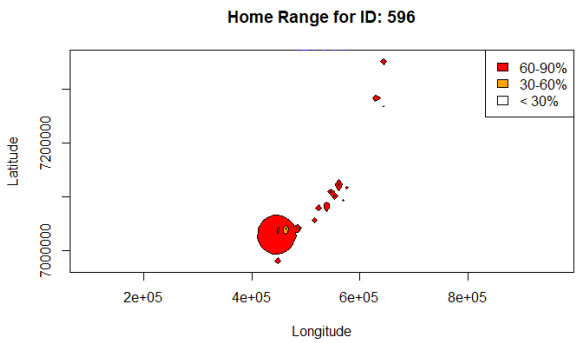
Home Range for ID: 596
60-90%
30-60%
< 30%
Latitude
7200000
7000000
2e+05
4e+05
6e+05
8e+05
Longitude

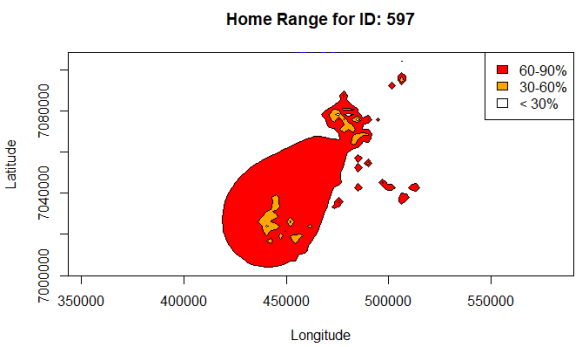
Home Range for ID: 597
60-90%
30-60%
< 30%
Latitude
7080000
7040000
7000000
350000
400000
450000
500000
550000
Longitude

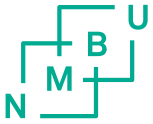

Norges miljø- og biovitenskapelige universitet
Noregs miljø- og biovitskapelege universitet
Norwegian University of Life Sciences

Postboks 5003
NO-1432 Ås
Norway